Spatio-temporal groundwater variations associated with climatic and anthropogenic impacts in South-West Western Australia.

K.X. Hu[a], J.L. Awange[a,b], M, Kuhn[a], A, Saleem[a]

[a] *School of Earth and Planetary, Spatial Science Discipline, Curtin University, Perth, Australia*

[b] *Geodetic Institute, Karlsruhe Institute of Technology, Engler-Strasse 7, D-76131, Karlsruhe, Germany*

Abstract

South-West Western Australia (SWWA) is a critical agricultural region that heavily relies on groundwater for domestic, agricultural and industrial use. However, the behaviours of groundwater associated with climate variability/change and anthropogenic impacts within this region are not well understood. This study investigates the spatio-temporal variability of groundwater in SWWA based on 2,997 boreholes over the past 36 years (1980-2015). Results identify the decline in groundwater level (13 mm/month) located in the central coastal region of SWWA (i.e., north and south of Perth) to be caused by anthropogenic impacts (primary factor) and climate variability/change (secondary). In detail, anthropogenic impacts are mainly attributed to substantial groundwater abstraction, e.g., hotspots (identified by above 7 m/month groundwater level change) mostly occur in the central coastal region, as well as close to dams and mines. Impacts of climate variability/change indicate that coupled ENSO and positive IOD cause low-level rainfall in the coastal regions, subsequently, affecting groundwater recharge. In addition, correlation between groundwater and rainfall is significant at 0.748 over the entire SWWA (at 95% confidence level). However, groundwater in northeastern mountainous regions hardly changes with rainfall because of very small amounts of rainfall (average 20-30 mm/month) in this region, potentially coupled with terrain and geological impacts. A marked division for groundwater bounded by the Darling and Gingin Scarps is found. This is likely due to the effects of the Darling fault, dams, central mountainous terrain and geology. For the region south of Perth and southern coastal regions, a hypothesis through multi-year analysis is postulated that rainfall of at least 60 and

65-70 mm/month, respectively, are required during the March-October rainfall period to recharge groundwater.

Keywords: Australia, groundwater, climate variability/change, anthropogenic impacts

1. Introduction

South-West Western Australia (SWWA; 28.5°-35.5°S; 114.5°-118°E, Fig 1), is an essential agricultural region of Western Australia that supports the livelihood of about 65% of its total population (1.7 million; *ABARES* 2018; *Population Australia* 2018). It relies heavily on rain-fed and irrigated agriculture, e.g., producing cereal crops such as wheat and canola besides sheep grazing for wool production (*ABARES*, 2018; *Hill et al.*, 2004). In the period 2016-2017, the gross value of agricultural production of Western Australia was $8.5 billion, of which 80% was exported to overseas markets (*Agriculture and Food*, 2018). Although this region is vital for its agricultural productivity, frequent droughts have caused heavy reliance on groundwater, which now accounts for about 75% of the total water usage in Western Australia (see, e.g., *CSIRO* 2009; *Ali et al.* 2012).

Groundwater is not only a valuable resource that supports agriculture, domestic water supplies and industries in Western Australia (*Taylor et al.*, 2013; *Tregoning et al.*, 2012). It also plays a crucial role in aquatic ecosystems that have interconnections with surface water (*Argent*, 2016). This feature allows ecosystems to maintain their functions by replenishing river and stream flows through groundwater during dry periods (*Kinal and Stoneman*, 2012). Many studies, e.g., *Barron et al.* (2011); *Dawes et al.* (2012); *Hughes et al.* (2012); *Kinal and Stoneman* (2012); *Ali et al.* (2012); *Eamus* (2015), indicate that groundwater levels are decreasing in SWWA due to decline in rainfall since 1975 on the one hand, and increased demands for water use on the other hand. For example, water levels in the Gnangara groundwater system have declined over the past 40 years due to over-abstraction (see, e.g., *Featherstone et al.* 2012; *Awange* 2012; *Awange and Kiema* 2013; *Department of Water* 2015; *Awange* 2018; *Awange and Kiema* 2019). The current decline and abstractions are not sustainable, i.e., natural recharge is not keeping pace with human abstraction (*Department of Water*, 2015). Anthropogenic impacts such as human abstraction, land use and land cover change (LULC) together with drier climate are exerting pressure on SWWA's groundwater (*CSIRO*, 2009). Accurate knowledge of spatio-temporal variability of SWWA's groundwater as well as impacts of climate variability/change and anthropogenic activities, therefore, is important for water

management, conservation, and to inform plans and policies governing its use.

However, understanding the spatio-temporal variability of groundwater can be challenging due to the limitations in groundwater data and their coarse spatio-temporal resolution. Currently, studies of groundwater variability are based on two main data sources; (i) local in-situ data (i.e., borehole data), e.g., *Hughes et al.* (2012); *Tweed et al.* (2007), and (ii), satellite-based Gravity Recovery and Climate Experiment (GRACE) data combined with hydrological or reanalysis models, e.g., *Strassberg et al.* (2009); *Leblance et al.* (2009); *Chen et al.* (2016); *Hu et al.* (2017). Generally, borehole data are more useful for temporal groundwater change analysis rather than study of its spatial variability (see, e.g., *Hughes et al.* 2012; *Tweed et al.* 2007) due to the complexity of spatial interpolation between boreholes, e.g., *Sun et al.* (2009). *Tregoning et al.* (2012) note that spatial interpolation of groundwater levels requires a large amount of data with sufficient density. Otherwise, the high spatial variability in the groundwater system and its complex storage dynamics make local measurements unsuitable for interpretation over a large area, and as such, introduces considerable uncertainties. GRACE-based groundwater spatio-temporal studies, on the one hand, are unable to capture the small-scale localized hydrological signals due to its coarse spatial resolution (*Awange et al.*, 2010, 2011). On the other hand, the uncertainties of meteorological forcing inputs in the associated hydrological models degrade their derived groundwater outputs (*Tregoning et al.*, 2012; *Bhanja et al.*, 2016).

In addition, climate variability/change produces significant impacts on groundwater recharge. Rainfall as the main source of groundwater strongly influences its spatio-temporal variations (*Hu et al.*, 2017), while rainfall itself is affected by climate variability/change, such as El Niño Southern Oscillation (ENSO) and Indian Ocean Dipole (IOD) (*Forootan et al.*, 2016). A relation between groundwater and ENSO/IOD may exist, e.g., *Holbrook et al.* (2009) indicate that ENSO cycles have impacts on the recharge of groundwater near the coastline (see, e.g., *Anyah et al.* 2018). Although anthropogenic impacts on groundwater are apparent over SWWA (*Department of Water*, 2015), previous studies mainly focused on hydro-chemical properties, such as the age of groundwater and pollution levels (e.g., *Suh et al.* 2003; *Han et al.* 2017), rather than providing spatio-

temporal details. Despite the requirement of spatio-temporal variability information on groundwater over SWWA to inform its sustainable use, studies that comprehensively undertake its analysis are currently lacking.

The aim of this study, therefore, is to undertake a spatio-temporal variability analysis of groundwater over SWWA over the past 36 years (1980-2015), through the exploitation of statistical methods of Man-Kendall test, cross-correlation, cross-validation, Kolmogorov-Smirnov test, and regression analysis to analyse 2,997 borehole and precipitation data in order to (i) assess the long-term and seasonal variability trends on the one hand, and the timing of low and high groundwater availability on the other hand, (ii) analyse spatial patterns of variations and recharge/discharge, and (iii), understand impacts of climate variability/change, and identify long-term anthropogenic impacts and "hotspots" (i.e., areas of substantial abstractions).

2. Study area: South-West region of Western Australia

The study area (South-West Western Australia; SWWA; Fig 1a) is selected based on the distribution of available boreholes (Figs 1b), with the northern part extending up to the town of Cervantes and the Yalgoo mountainous region (Figs 1c), and the southern part extending to the Albany coastline. Rainfall commences intermittently in March, but most of the annual rainfall falls between May and September (*CSIRO*, 2009; *Ali et al.*, 2012). There is a south-west to north-east decreasing gradient in annual rainfall from around 1200 mm along the south-west coast to 350 mm in the north-east mountainous areas (*CSIRO*, 2009). There is also a low inter-annual variability compared to other regions in Australia (*Nicholls et al.*, 1997; *CSIRO*, 2009). Previous studies, e.g., *Barron et al.* (2011); *Dawes et al.* (2012), indicate that the rainfall totals in SWWA decreased by around 20% between the late 1960s and early 1970s due to climate change and land cover changes. More details on rainfall in SWWA, such as the spatial patterns and trends can be found, e.g., in *CSIRO* (2009); *Ali et al.* (2012).

As for topographical features of SWWA, the Perth basin and Darling Plateau are divided by the Darling and Gingin Scarps (see Fig 1c). These two scarps affect groundwater behaviour since there is on average a 200 m difference in elevation across them. Also, different geological features (sandstones in the coastal plain and granite in the hills) to the west and east of these two major scarps affect groundwater recharge/discharge (see e.g, geology and hydrogeology in *CSIRO* 2009). However, since our study focuses only on groundwater behaviours (i.e., changes) and their relation to climatic and anthropogenic impacts, links to detailed geology and different aquifer formations are not discussed further here. In regions around Blackwood Plateau (Fig 1c), Whicher Scarp to the north and Barlee Scarp to the south exist. Generally, elevation changes are highest in the northeast and lowest in the southwest for SWWA, and the groundwater naturally flows from the eastern sides of the Darling and Gingin Scarps into the coastal plains due to the effects of the hydraulic gradient (see Fig 1c).

The Gnangara groundwater system provides the most substantial groundwater, supporting almost 50-60% of the water use in SWWA (see location in Fig 1c, *Skurray et al.*

2012; *Department of Water* 2015). However, *Awange* (2012); *Awange and Kiema* (2013); *Department of Water* (2015); *Awange* (2018); *Awange and Kiema* (2019) indicate that many parts of the Gnangara system are currently over-allocated and the groundwater level has declined continuously over the past 40 years. On the one hand, this situation creates significant pressure on and risk to local ecosystems. On the other hand, there are many dams located along the eastern side of the central Darling Scarp (see Fig 1c), which provide resources for domestic water use, acting as artificial buffers. They play an important role in storing water during low demand in the rainy seasons and then discharging them during dry periods. These dams may have an influence on groundwater in the nearby regions due to the fact that there exist interconnection between groundwater and surface water. This interconnection is considered to be an anthropogenic impact, given that nearby groundwater levels tend to follow variations in the dam levels.

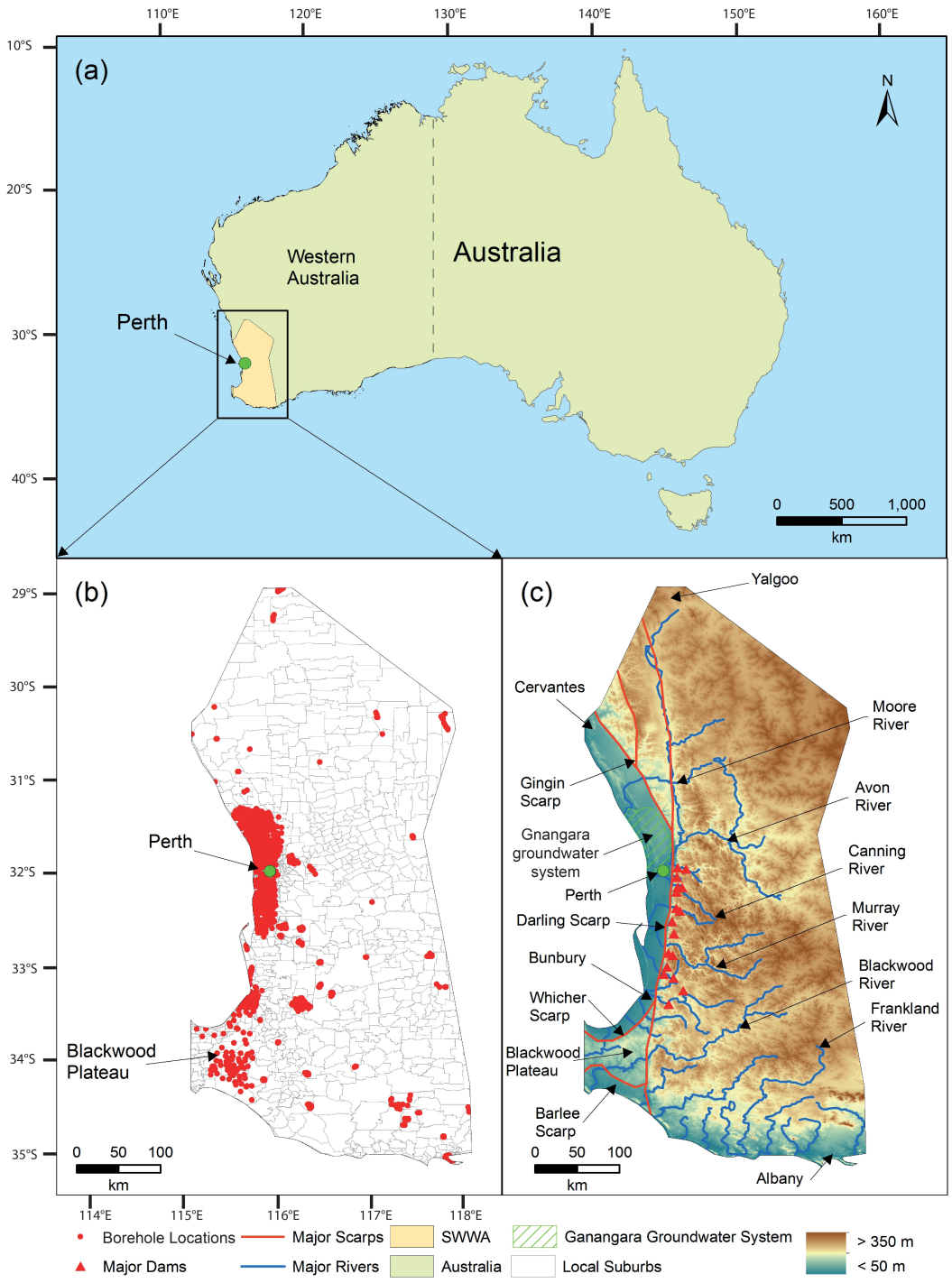

Figure 1: Spatial features of SWWA; (a) location, (b) borehole distribution, and (c) major dams, rivers, scarps, and elevation, as well as the location of the Gnangara groundwater system. A high density of borehole data exists to the north and south of Perth, as well as Bunbury and the Blackwood Plateau. Darling and Gingin Scarps and many dams in the central SWWA affect groundwater behaviour between the coast and mountainous regions. Pannel (c) is reproduced and modified according to *CSIRO* (2009) and *Ali et al.* (2012).

3. Data and methods

3.1. Data

3.1.1. Borehole data

Borehole data are acquired from "The Australian Groundwater Explorer", which is a web-based mapping application (see online: http://www.bom.gov.au/water/groundwater/explorer/) that provides groundwater level monitoring information. All downloaded available records date back to approximately 1900, while most data are after preprocessing concentrated within the 1980-2015 period. For further processing data from only this period have been considered. The groundwater level for each borehole is in daily format, instantaneous and discontinuous records, and therefore requires preprocessing into monthly, continuous records (see Section 3.2.1). The standing (or static) water level (SWL; representing measurements from the reference point on the bore, e.g., the top of casing, to the groundwater table; see detailed explanation at http://www.bom.gov.au/water/groundwater/explorer/faq.shtml) is selected to investigate spatio-temporal variations of groundwater. In addition, this study is only concerned with the variation of the SWL irrespective of the borehole's depth and the surrounding geology. This is due to the fact that our study mixes data for different aquifers and different depths, and as such could lead to erroneous interpretations between groundwater changes and geology.

3.1.2. Rainfall products

Bureau of Meteorology (BoM) rainfall data with spatial 0.25° (1980-2006), 0.05° (2007-2015) and monthly temporal resolutions are available from the Australian Government. The BoM data are generated by interpolating rain-gauge stations Australia-wide and is considered the most reliable rainfall product in Australia (*Fleming et al.*, 2011; *Fleming and Awange*, 2013). Besides, use is made of the Multi-Source Weighted-Ensemble Precipitation (MSWEP), available from 1980 to 2015. MSWEP is a global rainfall dataset with 0.1° and monthly spatial and temporal resolutions, respectively. Version 2.1 of the MSWEP product validated for Australia by *Awange et al.* (2019)

merges the highest quality rainfall data sources (BoM is not included in MSWEP, *Beck et al.* 2017a,b), and as such are used to check the consistency of BoM products used in this study. Here, the BoM data for the period 2007-2015 with 0.05° spatial resolution are re-scaled to a resolution of 0.25° in order to match the spatial resolution with the previous period of 1980-2006. MSWEP data are also re-scaled to a resolution of 0.25° to match those of BoM. The results show that there is almost no difference (average 2.5 mm monthly difference and 0.997 correlation at 95% confidence level) between the BoM and MSWEP datasets over SWWA. Similar results between BoM and Tropical Rainfall Measuring Mission (TRMM) 3B43 are also found in *Fleming et al.* (2011); *Fleming and Awange* (2013), thus indicating the consistency of the BoM rainfall product, which is subsequently used in this study. The monthly BoM data are downloaded from http://www.bom.gov.au/jsp/awap/rain/archive.jsp?colour=colour&map=totals&period=month&area=nat, while the MSWEP data are downloaded from http://www.gloh2o.org/.

3.1.3. Climate indices

Multivariate El Niño-Southern Oscillation Index - (MEI) is derived from tropical Pacific COADS (Comprehensive Ocean-Atmosphere Data Set) records, which is a combination of six observed variables over the tropical Pacific and includes sea-level pressure, surface zonal, and meridional wind components, sea surface temperature, and cloudiness (*Wolter and Timlin*, 1998). The Dipole Mode Index (DMI) measures the difference between the area mean sea surface temperature anomalies in the IODW (western equatorial Indian Ocean; 50°E-70°E and 10°S-10°N) and IODE (southeastern equatorial Indian Ocean; 90°E-110°E and 10°S-0°N, *Saji and Yamagata* 2003; *Cai et al.* 2011), which is used to monitor the Indian Ocean Dipole (IOD). In this study, MEI and DMI are compared to BoM rainfall, and borehole derived groundwater variations in order to assess climate variability/change impacts on groundwater for the 1980-2015 period.

3.2. Methods

This section presents the pre-processing steps for the borehole data and the subsequent analysis methods employed.

3.2.1. Borehole data pre-processing

The downloaded borehole groundwater level data are pre-processed in 3 steps to obtain continuous records between 1980 and 2015 as described below:

1. **Data cleaning and selection**: Duplicate data are removed, and only the standing water level (SWL) measurements of groundwater are selected for further analysis.

2. **Generate monthly data**: Convert daily instantaneous records into monthly by averaging all available daily data for a particular month. The monthly data may still be discontinuous because of missing records leading to unequal weight and bias when analyzing average monthly groundwater variations.

3. **Select data with continuous 12 months' records in a year scale**: Retain monthly data only if the 12 months' records are complete in a year.

After pre-processing, records from a total of 2,997 out of 3540 borehole stations (i.e., around 85% of the data) are used. Note, however, that most of the borehole records only cover 1 to 3 years within the study period 1980-2015, with only a few boreholes covering more than 10 years. When using various merging or interpolation methods (see details of interpolation methods in Section 3.2.3) to capture the spatio-temporal variations and trends over the 36 years in SWWA, uncertainties and biases cannot be avoided and are, therefore, discussed in the results Section 4.4.

3.2.2. Monthly anomalies

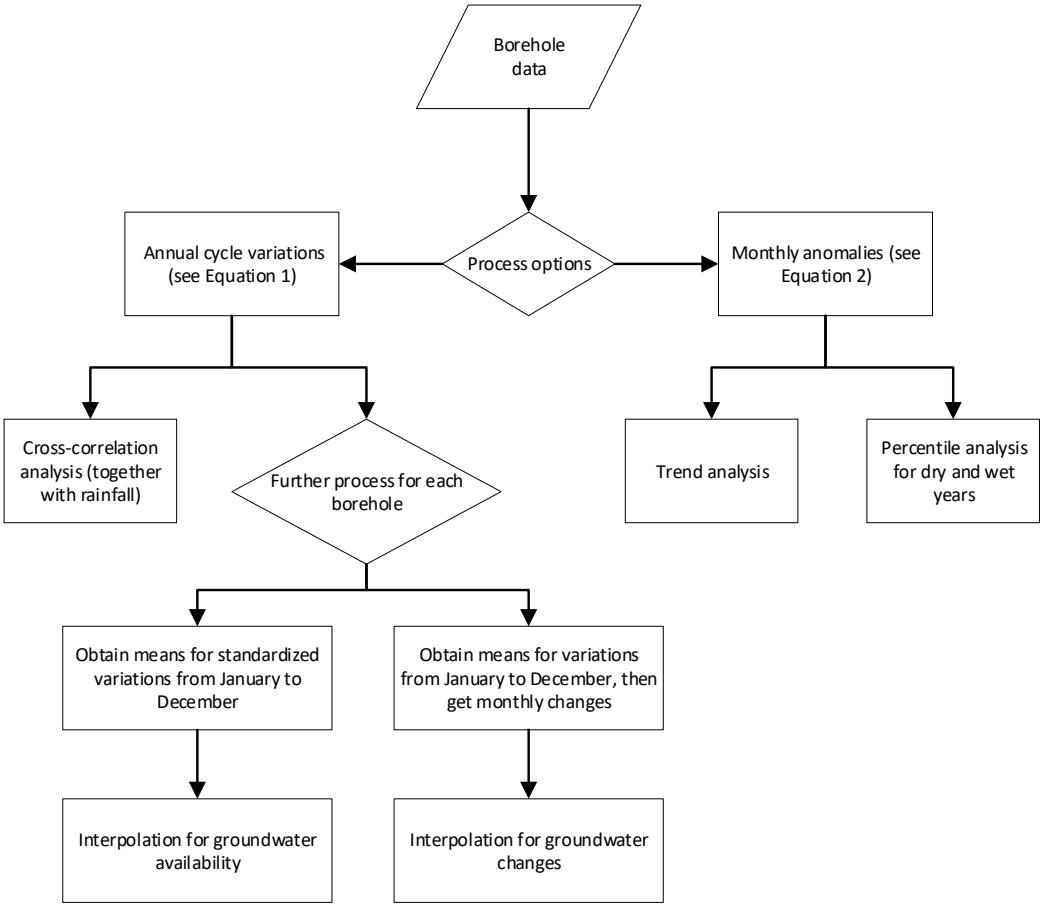

Figure 2: Analysis and processing steps of borehole data.

Figure 2 presents the analysis and processing flow chart of borehole data. Here, borehole data are processed in two slightly different ways: (1) inter-annual variation of annual cycles (referred here as "annual cycle variation" as a short hand) to analyze changes of the annual cycle over time (e.g. from year-to-year), and (2), monthly anomalies with respect to the long-term mean (i.e., 1980-2015) to analyse long-term trends. Both quantities are standardized (see details below) for ease of comparison between ground water and rainfall data. Furthermore, results from (1) are used to spatially interpolate average monthly patterns of ground water availability and change.

Annual cycle variations for groundwater data are derived from monthly averages for

a particular year by subtracting the average of that year, e.g.

$$y_m^{(i)} = -(y_i - \bar{y}_a); i = 1, ..., 12. \quad (1)$$

In Equation 1, y_i are monthly averages where the index i indicates the month starting with $i = 1$ for January and $\bar{y}_a$ is the average of all monthly values in a particular year. The differences $y_m^{(i)}$ taken between y_i and $\bar{y}_a$ for each month, are used to characterise the annual cycle for a particular year. The negative sign on the right-hand side of Equation 1 has been introduced to convert borehole observations (positive downwards) to SWL values (positive upwards). Applying this principle to individual borehole records results in annual cycle variations for each borehole. It is worth mentioning that the quantities $y_m^{(i)}$ do not contain a long-term trend and variations (e.g. beyond one year), thus they are considered here to be better suited to study inter-annual variations. Furthermore, the same principle is applied to rainfall data, though without the negative sign as described above.

Monthly anomalies for groundwater data are derived from monthly averages by subtracting the long-term average (i.e., 1980-2015), e.g.,

$$y_{ma}^{(i)} = -(y_i - \bar{y}_p); i = 1, ..., N \times 12. \quad (2)$$

In Equation 2, $\bar{y}_p$ is the long-term average for the complete data period considered. The monthly anomalies $y_{ma}^{(i)}$, taken between y_i and $\bar{y}_p$ for each month, are used to characterize long-term changes (e.g. trends or variations). Note that the index i is now running until $N \times 12$, with N being the number of years covered by a borehole record. Again, the negative on the right-hand side of Equation 2 follows the same reasoning as given above and all monthly anomalies are averaged to obtain average monthly anomalies (for SWWA or a sub-region). It is worth mentioning that the quantities $y_{ma}^{(i)}$ preserve the long-term trends and variations, thus are used here to derive linear trends.

The quantities $y_m^{(i)}$ and $y_{ma}^{(i)}$ are further used to derive spatial averages over a given region (either SWWA or a sub-region) and standardized to obtain average annual cycle

variations or average monthly anomalies (see Fig 3). The standardization has been done by, e.g.,

$$Z = \frac{X - \mu}{\sigma} \tag{3}$$

where X is the value that is being standardized, μ the mean of the distribution and σ the standard deviation of the distribution.

In addition, cross-correlation (*Knapp and Carter*, 1976) measures the similarity between one vector and shifted (lagged) copies of another vector as a function of the lag. In this study, cross-correlation is used to examine the relationships between groundwater and rainfall from the results of $y_m^{(i)}$. The lags are obtained between rainfall and groundwater when two variables reaches the maximum correlation. Linear trends are tested and calculated from the results of $y_{ma}^{(i)}$ using Mann-Kendall (MK) test (*Mann*, 1945) and ordinary least-squares method. At last, percentiles are calculated for both groundwater and rainfall from the results of $y_{ma}^{(i)}$ to identify drought years for the SWWA. Years with below the 25th percentile are identifer as dry years, while those above 75th are identified as wet years, see detailed method in *Awange et al.* (2008).

In order to illustrate the procedure to derive annual cycle variations, Fig 3a provides 4 randomly selected boreholes as an example for all boreholes in SWWA. One can see that these borehole data cannot even fully cover a 5-year period, thus, the data coverage for different boreholes for the 1980-2015 period is expected to be fragmented. From Figs 3a to 3b, the annual mean for each borehole is removed according to Equation 1. Since the standing water level (SWL) represents the distance from reference points (surface in most cases) to the groundwater table, the time series in Fig 3b are inverted by considering the negative sign of the values in Fig 3a in order to correctly show increasing and decreasing trends. Finally, as shown in Fig 3c, all annual cycle variations are spatially averaged and subsequently standardized for ease of comparison to other products such as rainfall.

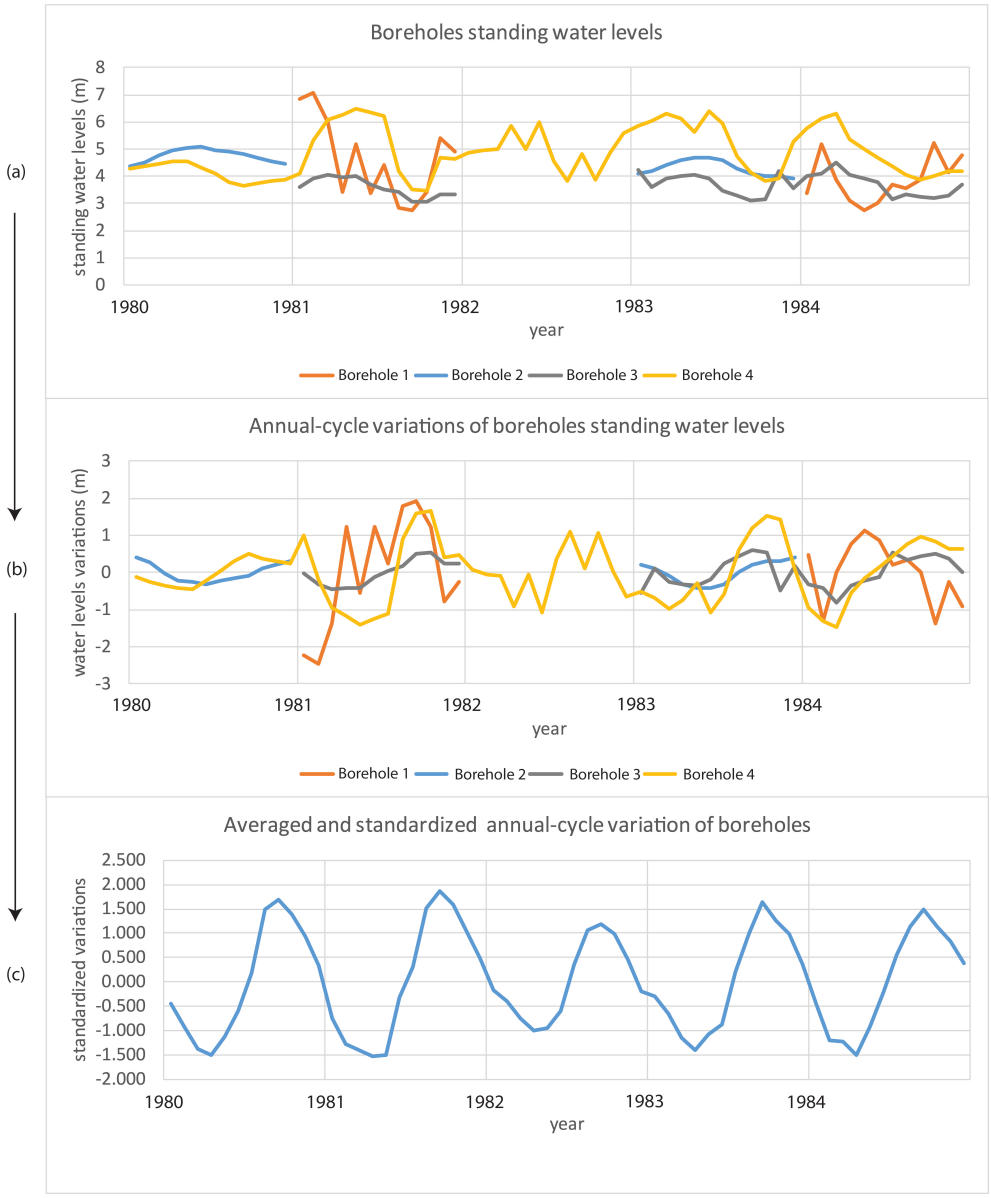

Figure 3: Illustration of the derivation of annual cycle variation from 1980-1984. (a) the original boreholes standing water levels, (b) borehole with the annual mean for each year removed using Equation 1, and (c), average of all boreholes variations and the derived standardized time series. Note that only 4 boreholes are shown as examples in (a) and (b) to represent all boreholes in SWWA, while the time series in (c) represents the final results averaged from 2,997 boreholes.

3.2.3. Spatial interpolation

To see spatial patterns of groundwater availability and groundwater changes, borehole data (see previous Section 3.2.2) are interpolated using two different interpolation meth-

ods; the Inverse Distance Weighted (IDW; *Philip and Watson.* 1982) and Kriging (*Oliver*, 1990). Both methods have been used to spatially interpolate groundwater in previous studies, e.g., *Sun et al.* (2009); *Nikroo et al.* (2008). To assess the performance of the two interpolation methods, their results are compared using cross-validation (e.g., *Robinson and Metternicht* 2006), the two-sample Kolmogorov-Smirnov (K-S) test (*Massey*, 1951; *Awange et al.*, 2016; *Saleem and Awange*, 2019), and regression analysis. Note that these validation methods are applied only to the boreholes in the regions north and south of Perth (having high data density, see Fig 1b) due to the fact that the other regions have insufficient data coverage, thus are not suited to test the performance of the interpolation techniques.

In detail, 594 random points (around 1/3 of the total boreholes in the selected regions are extracted and used for the Kolmogorov-Smirnov test as well as for cross-validation. As shown in Fig 4a, both the IDW and Kriging interpolation results follow the same cumulative distribution at the 95% confidence level with a k-value of 0.05, which indicates that the two interpolation methods deliver acceptably similar results. However, the K-S test shows the IDW interpolated data to be closer to the original dataset. The cross-validation results (Fig 4b) also show IDW to have similar performance to Kriging, but with better-interpolated values that have lower root-mean-square-errors (RMSEs, i.e., IDW/Kriging interpolated values compared to the nearest points of original values) of 0.48, compared to 0.53 for Kriging. Both the RMSEs for IDW and Kriging gradually become stable (decreasing rate smaller than 0.005 per 10 points) around 580 points, which indicates that the used 594 points are sufficient for validation. Out of the total 594 locations tested, there are around 70% points showing that IDW has smaller errors compared to the Kriging method. Following these assessment results, in Section 4.2, only interpolation results using the IDW method are presented and discussed further.

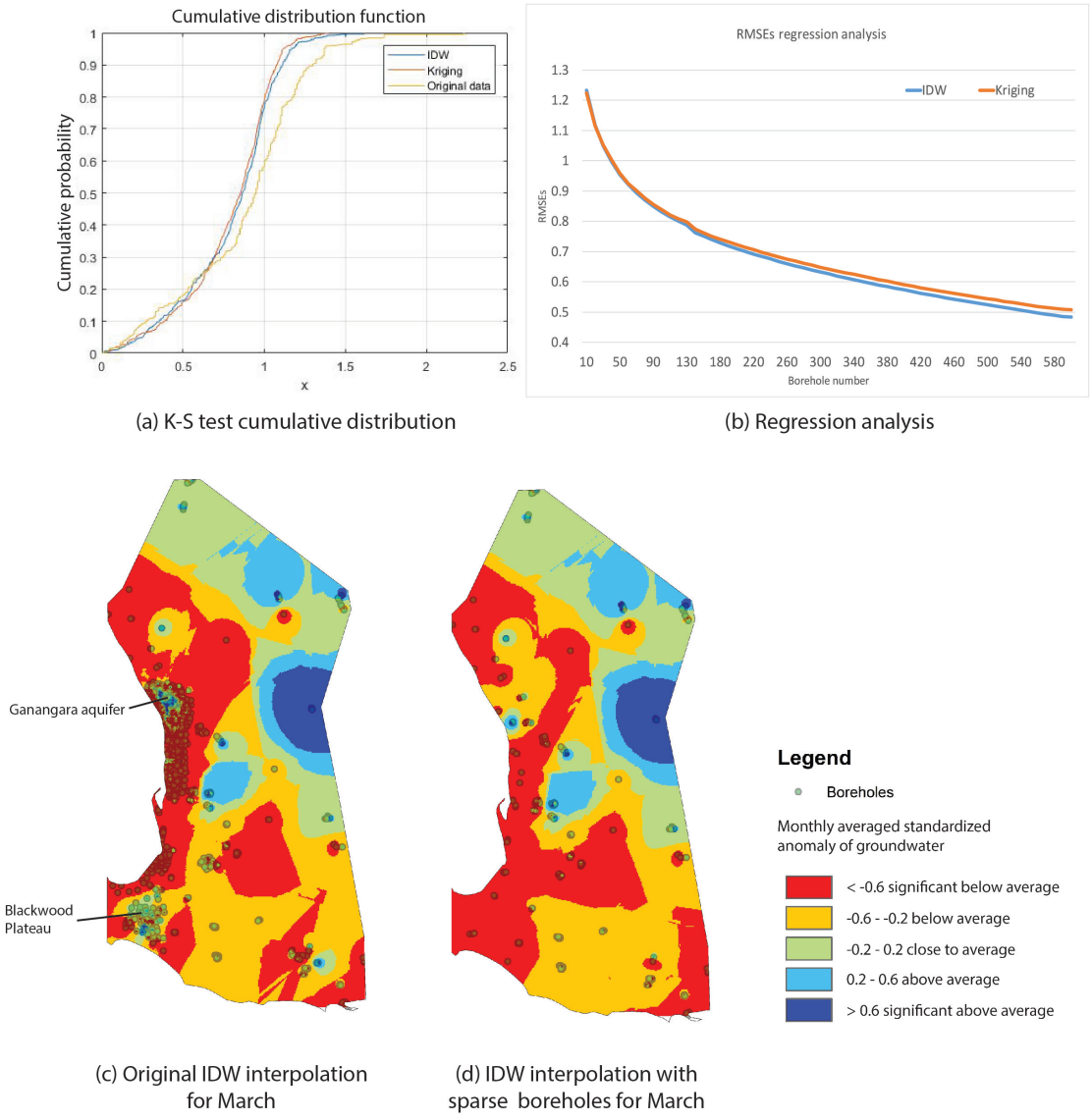

(a) K-S test cumulative distribution

(b) Regression analysis

(c) Original IDW interpolation for March

(d) IDW interpolation with sparse boreholes for March

Figure 4: Validation results for IDW and Kriging interpolation methods for the regions north and south of Perth and uncertainty simulation for sparse borehole interpolations: (a) Cumulative distribution comparison of 594 randomly generated points (IDW and Kriging) and the nearest original data; (b) regression analysis of both IDW and Kriging, RMSEs gradually decrease with increasing number of points used; (c) IDW interpolation for groundwater availability (March is randomly selected), and (d), the same IDW interpolation as (c) but using sparse boreholes. From (a)and (b), the results show that both IDW and Kriging have similar interpolated values, where IDW provides results that are relatively closer to the original dataset and hence used for further analysis. From (c) and (d), the interpolation results in Blackwood Plateau and Gnangara groundwater system are significantly affected by using different borehole densities.

Since the eastern side of the Darling Scarp has a sparse distribution of boreholes, the interpolation results are less reliable compared to those of high density areas. To roughly estimate the uncertainty in areas with sparse borehole distributions, the western side's high-density boreholes are randomly reduced to roughly match the density of the eastern side of the Darling Scarp (30-40 boreholes per degree cell). The IDW interpolation results using the original boreholes (Fig 4c) and those using the reduced sparse boreholes (Fig 4d) are then compared.

The comparison results indicate that major differences are present over the Blackwood Plateau and Gnangara groundwater system, where the number of boreholes used significantly affected the outputs of interpolation. It is most likely that these two regions' groundwater have features that are highly variable, i.e., caused by complex geological, topographic and anthropogenic conditions. For example, *Departement of Water* (2009) indicate that many types of aquifers located in Blackwood Plateau and their depths varies from several meters to hundreds of meters. Taking reference from the western side of Darling Scarp, the uncertainties in the eastern side of the mountainous areas (i.e., those interpolation areas with no borehole control) are expected to be large, due to the fact that mountainous areas' hydrogeological conditions are usually more complex than that of the coastal plain.

3.2.4. Identification of anthropogenic hotspots

The month to month (current month compared to the previous month, see Section 3.2.2) changes in groundwater levels are calculated for all available borehole records to identify potential anthropogenic hotspots. This interpretation is based on the expectation that groundwater level variation (recharge/discharge) should generally exhibit gradual change. A certain area's groundwater change falling outside an expected change may, therefore, likely have resulted from anthropogenic impacts though other impacts cannot be fully excluded. Specifically, the chance of month to month changes in groundwater level over n meters (e.g., $n = 1$ m, 2 m, 3 m ...) is separately calculated as:

$$F_n = MMC_n/MMC_t \times 100\%; \quad n = 1, 2, 3, ..., \tag{4}$$

where F_n are the chances of month to month changes of groundwater level above n meters for all boreholes, while MMC_n and MMC_t represent the number of records over n meters and total number of records for all boreholes, respectively.

In order to apply Equation 4, a threshold value x ($x \epsilon n$ meters) needs to be defined upon which a "hotspot" is identified. To do this, an example is used as an illustration. Assuming there are 100 month to month changes of groundwater level records for all boreholes in the studied region, and only 1 record shows a change above x meters; where $x \epsilon n$. Then the chance of groundwater level change over x m is 1% according to Equation 4, meaning that this change rarely occurs within the study regions. This x meters, thus, can be regarded as the threshold that identifies "hotspots".

Following the example illustrated above, all borehole data in the study region are analysed to determine the threshold x for which the change is equal or less than 1% in order to obtain a 99% confidence level. This confidence level incorporates the possibility that abnormal groundwater level changes could also occur due to irregular rainfall, special geological and topographic conditions, as well as anthropogenic impacts. In addition, it should be noted that minor human abstractions are difficult to detect using monthly data, since the recovery time could be short based on the amount of abstraction and the change of groundwater may be too small to be distinguished from other natural changes. Thus, the 1% is selected to detect more substantial anthropogenic impacts (e.g., abstractions). In this study, month to month groundwater changes of less than 1 meter account for 73.6% of all records in SWWA, whereas those of 6 meters account for around 1%, and those for 7 meters and above, less than 1%. From this, therefore, boreholes with groundwater changes over 7 meters resulting from month to month change analysis are identified as anthropogenic "hotspots" within SWWA, i.e., $x = 7$ meters.

Next, for those single boreholes with groundwater level changes above 7 meters, the chance of 7 meters is also calculated for each of them using Equation 4, in order to see how frequently such anthropogenic impacts occur, e.g., if a borehole has 36 monthly

change records, and only 1 shows above 7 meters change from month to month, this means that anthropogenic impacts rarely occur in this borehole since the chance is 1/36.

4. Results and Discussion

4.1. Temporal analysis

An overview of the temporal analysis is presented in Fig 5 showing monthly averages of groundwater and rainfall in relation to the climate indices MEI and DMI. In particular Fig, 5a shows standardized anomalies of groundwater and rainfall time series with long-term mean removed, as well as those of two climate indices (MEI and DMI) for examining impacts of ENSO and IOD, respectively. Figure 5b shows annual cycle variation of groundwater and rainfall. The available numbers of used boreholes are also presented, and helps infer confidence levels for the derived groundwater time series. Figure 5c identifies dry (below 25th percentile) and wet (above 75th percentile) periods in comparison to annual rainfall. Finally, correlations and time delays (lags) between rainfall and groundwater are shown for each year in Fig 5d.

SWWA's groundwater variability follows a relative uniform intra-annual pattern based on the data in Fig 5b, with periods of mostly increasing levels from May or June to August or September, and periods of decreasing levels in the remaining months of each year. Even though, variations in 1999 are derived from only 10 borehole stations, it appears to show no significant difference from the other years. Furthermore, groundwater variations follow rainfall variations to a large extent, with correlations consistently around 0.6-0.8 (with an average of 0.74 over the entire study period) and 1-3 month(s) lag (with an average of 2 months' lag) for each year as seen in Fig 5d, corroborating the results of *Rieser et al.* (2010) who also obtained similar correlations and lags between rainfall and total water storage (comprising also of groundwater) over the whole of Australia.

4.1.1. Climate impacts on groundwater level

A significant continuously decreasing trend in groundwater levels from 2000 is detected and is apparent from Figs 5a and 5c, with an average reduction of 13 mm/month (or 156 mm/year). This may be partly attributed to the continued low level of rainfall (see Fig 5c). Since 2000, most years have been identified as moderately dry or dry years (2001, 2002, 2004, 2006, 2007, 2009, 2010, 2012, 2014 and 2015; i.e., 10 out of 16 years) with

annual rainfall close to or below the 25th percentile. Many studies have reported most of these years as the "Australian Millennium Drought" (see, e.g., *Cai et al.* 2014; *Heberger* 2011). The rainfall trend between 2000-2015 is stable, however, with a 40 mm decrease in annual total values compared to previous periods (i.e., 560 mm compared to 520 mm). Based on the comparison between annual and seasonal rainfall (May - September) in Fig 5c, there is an almost consistent difference (100 - 150 mm) between them, indicating the decline of annual rainfall to be due to the decline in seasonal rainfall.

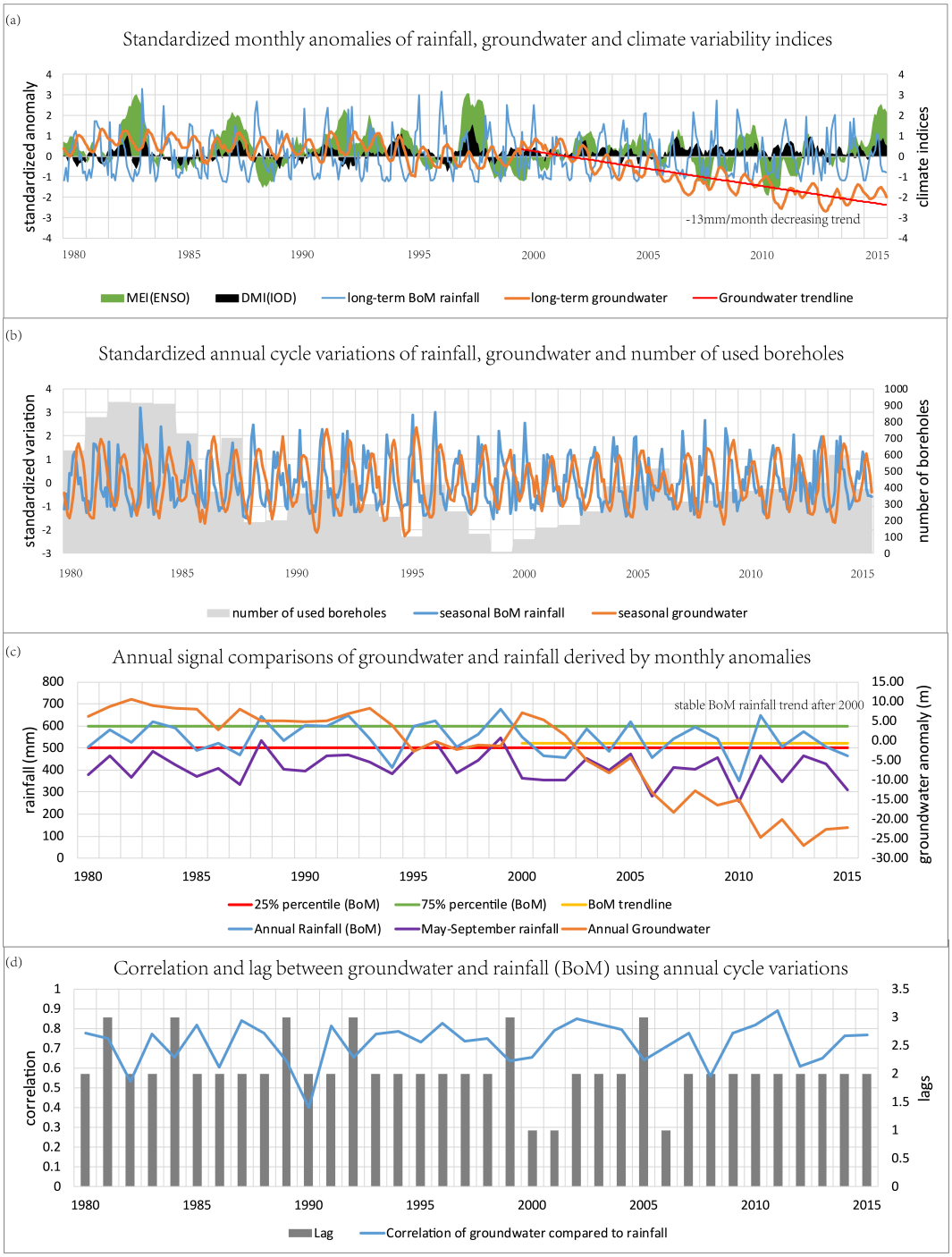

Figure 5: Groundwater temporal analysis in comparison to rainfall and climate indices; (a) standardized monthly anomalies of rainfall, groundwater and climate variability indices, (b) standardized annual cycle variations of groundwater, rainfall and number of used boreholes, (c) annual signals' comparison of groundwater and rainfall derived by monthly anomalies, and (d), correlations and lags between groundwater and rainfall (BoM) using annual cycle variations. Note that the results are biased towards the north and south of Perth areas with a higher density of borehole data (see boreholes' distribution in Fig 1b). The linear trend in (a) is significant (95% confidence level) when tested using Mann-Kendall, while the trend in (c) is not. The results show that the decline in groundwater level is partly due to low level rainfall since 2000.

On the one hand, rainfall is also affected by atmospheric and ocean interactions such as ENSO and IOD. Figure 5a indicates that SWWA's rainfall has a similar rainfall cycle to ENSO over a period of approximately 7 years (*Tudhope et al.*, 2001; *Li et al.*, 2013; *Niedzielski*, 2014), e.g., 1982-1987, 1988-1994, 1995-2001, 2002-2010. In addition, most of the moderately dry or dry years since 2000 listed above have been labelled by BoM as El Niño years (see online records at http://www.bom.gov.au/climate/enso/enlist/), which are known to bring low levels of rainfall throughout most of Australia.

On the other hand, according to *Ashok et al.* (2003), IOD has been found to have significant impacts on the winter rainfall (June, July, August) of western and southern Australia. A positive IOD produces a drier climate than average during winter-spring (Fig 5a shows IOD as continuously positive since 2000), and a wetter climate in summer. A negative IOD impact on rainfall is not apparent in SWWA according to BoM statistics (http://www.bom.gov.au/climate/iod/#tabs=Negative-IOD-impacts). Therefore, under both effects of ENSO and a positive IOD, continuous low levels of rainfall may be one of the contributing factors to the decline in groundwater levels experienced since 2000. La Niña events brought above average rainfall in 2008 and 2011 (see Figs 5a, b and c; also see La Niña records on BoM website: http://www.bom.gov.au/climate/enso/lnlist/), years during which the groundwater balance returned to positive (inflow was greater than abstraction and outflow). However, there was no significant effect on the long-term decline because of a lack of consistent high rainfall years (e.g., one "good year" is not good enough to replenish groundwater).

4.1.2. Anthropogenic impacts on groundwater level

The continuous low levels of rainfall after 2000 is one of the causes for the decline of groundwater levels in SWWA. However, anthropogenic impacts, such as human abstraction is also a contributing factor. For example, the stable annual rainfall trend for the 2000-2010 period does not fully correlate with the increasingly declining trend of groundwater in Fig 5c. Groundwater levels instead, drop on average around 20 m from 2000 to 2015 (but this may be mostly attributed to data from north and south of Perth, which are biased towards those areas in the spatial distribution). Similar results are mentioned

e.g., in *Featherstone et al.* (2012), who conclude that Perth's basin groundwater levels dropped due to anthropogenic impacts. Further evidence for a major anthropogenic influence is the fact that rainfall variations between the period 1983-1988 and 1999-2004 (see, Fig 5c) are largely similar in terms of trends and magnitudes, but groundwater behaviour within these two periods are entirely different (i.e., stable over period 1983-1988 but decreasing over the period 1999-2004).

Annual cycle variations (see Fig 5b) show that groundwater varies according to rainfall, with the correlation from 2000-2015 between them being 0.748, with an average 2 months' lag. The annual groundwater level (Fig 5c), however, shows a variety of responses to annual rainfall, including a stable level before 1993. After that, groundwater reaches a new low level due to a 2-year drought (from late 1993 to early 1995), and then it appears to recover after 2 years' wet conditions (late 1998 to early 2000). After 2000, groundwater declines slowly as the 'Millenium' drought starts. During the same time, groundwater abstraction increased significantly due to increased groundwater usage and population growth. For example, groundwater usage in 1985 was around 500 GLs/year according to *Department of Water* (2007), this usage tripled in 2005. Moreover, around 500,000 population moved to Western Australia between 2000 and 2010 about double the rate than in the period 1980-2000 (*Alexander*, 2018). Although the *Department of Water* (2007) indicates that the sustainable groundwater usage for Perth basin is 1937 GLs/year and allocation limit is 1472 GLs/year, the groundwater balance (see, Fig 5a or c) had already significantly decreased after 2002 with groundwater usage of around 1300-1400 GLs/year. This overestimation of sustainable groundwater usage in annual water report is possibly due to the high rainfall value of 2007. Overall, climatic factors seem to have weaker impacts compared to anthropogenic activities that have significant effects on the decline of groundwater after 2000.

4.2. Monthly average spatio-temporal pattern analysis

For a more detailed analysis of the impacts of rainfall on groundwater, monthly averaged rainfall (Fig 6a) are compared with spatially interpolated monthly averaged groundwater anomalies (Figs 6b and 6c) for each month. Figure 6a uses colour gradients to

display details in the spatial distribution of rainfall over the study region. Figure 6b shows the averaged groundwater level changes for each month compared to those of the previous month (e.g. difference previous month minus present month). A threshold of ± 0.2 m is set through multiple tests in order to clearly show the spatial gradients of the recharge/discharge distribution. Figure 6c presents the monthly averaged standardized groundwater anomalies. Based on the natural breaks classification method (*Jenks*, 1967), five classes are established to show groundwater levels in comparison to the annual average level, namely (i) significantly below average, (ii) significantly above average, (iii) below average, (iv) above average, and (v), close to average (Fig 6c).

4.2.1. Rainfall patterns

Figure 6a indicates an increasing gradient for rainfall from north-east to the south-west for most months, except January, February, and March. January is the only month that clearly shows higher rainfall in the eastern mountainous areas of SWWA than in the coastal areas, though, with rather low levels. From March, rainfall gradually increases along the southern coastline of the study region. From April to November, the spatial patterns of rainfall are approximately the same, in which the Darling and Gingin Scarps roughly act as boundaries with most of the rainfall occurring in the coastal plain. During the rainy season (May to September), major rainfall are received in regions south of Perth, Bunbury and the Blackwood Plateau (see locations in Fig 1c). Finally, the rainfall in December displays a north-south dipole pattern with relatively low levels.

4.2.2. Groundwater recharge/discharge patterns

In order to understand the relationships between rainfall and groundwater recharge/discharge, the concept of lag between rainfall and groundwater needs to be well understood. In Section 4.1, we stated that an average 2 months' lag exists between the time it starts to rain and groundwater starts to recharge (in agreement with *Rieser et al.* 2010). This is usually misunderstood to mean rainfall needs to take two months' time to penetrate soils, rocks and finally become groundwater. In actual sense, a detailed water balance has to be considered, which takes into account the fact that rainfall needs to reach a

threshold value in order to recharge groundwater. For example, when rainfall reaches the ground, it has to satisfy the soil and plant transpiration first (*Alley*, 2009) before the recharge process can begin, where the excess part takes some time (the lag) to infiltrate through soils and rocks and finally reaches the groundwater table. At this moment, only if the amount of excess rainfall (i.e., groundwater input) is greater than the amount of groundwater outflow (i.e., groundwater output, e.g., from human abstraction or natural discharge such as into the ocean), does the groundwater recharges (i.e., groundwater level raises). In other word, if the rainfall does not reach a certain threshold value, i.e., continuous low rainfall level, there will be no lag (i.e., infinite lags) since the groundwater will never recharge.

Comparing the spatial patterns of groundwater recharge/discharge to spatial rainfall in Figs 6a and 6b, both lag and threshold conditions exist, i.e.,

(i) For most of the coastal regions of SWWA, there appears to be less than one month's lag between rainfall and groundwater. For example, one can see that rainfall gradually increases along the southern coastline of the study region in March (Fig 6a), while groundwater is still discharging (Fig 6b). Similar to April, more rainfall arrives at southern coastline and south of Perth region, while groundwater level still shows decline. During these two months, groundwater levels continue to drop because the total recharge from rainfall (50 mm for south of Perth and 65 mm for southern coastline in April, see Fig 6a) is less than the total of all discharges (i.e., not sufficient to satisfy soil and plant transpiration, as well as groundwater outflow). In May, however, the rainfall value reaches around 120-130 mm and the groundwater balance instantly becomes positive (i.e., groundwater level raises, see Fig 6b). Similarly from October to November, when rainfall amount falls from 70 to 50 mm in southern coastline (from 60 to 45 mm in south of Perth), the groundwater balance instantly becomes negative (i.e., groundwater level drops). Thus, a minimum of 65-70 mm/month of rainfall is postulated here as the threshold needed to maintain groundwater balance in the southern coastal region of SWWA, and around 60 mm/month for south of Perth.

(ii) One to two month(s)' lag between rainfall and groundwater exists in regions north of Perth (Gnangara groundwater system) and Blackwood Plateau. For example, rainfall during May reaches 120-130 mm already for both regions (see Fig 6a), whereas the groundwater in these two regions are still mainly discharging (see Fig 6b). This groundwater pattern is different compared to other coastal regions (i.e., south of Perth), where most areas are starting to recharge from May. In June-July, over half of north of Perth and Blackwood Plateau's groundwater start to recharge, then discharge in November (October for other regions, rainfall in November is 35-40 mm for both regions, north of Perth and Blackwood Plateau). Due to this obvious lag, we cannot identify the threshold value of rainfall recharging groundwater and as such, in (i), there is a small portion of north of Perth's groundwater that in discharging in May with rainfall around 180 mm, while in October, most of north of Perth's groundwater is recharging with rainfall at only 50-60 mm. Finally, this lag is most likely caused by geological conditions, e.g., large but low infiltration aquifers receive groundwater flow from other regions during the dry period, while other regions mostly rely on recharge of rainfall.

Although, the results in Figs 6a and 6b show some consistencies across the western coastal regions of SWWA, in the mountainous regions, however, rainfall does not appear to be correlated to groundwater for most months, making it hard to identify lags and thresholds between rainfall and groundwater. For example, even with only the rainfall amount in January being around 20-25 mm over the northeastern mountainous regions, the groundwater level is increasing (see, Fig 6b). Higher rainfall (40-80 mm) arrives in this region during June, however, but in contrast to January, groundwater levels are decreasing. This is possibly due to (i) the mountainous region's groundwater variations mainly depend on the groundwater flow itself, (ii) terrain effects make surface water gather in valleys and quickly flows away (e.g., *Crissa and Davissonb* 1996), as well as (iii), high evaporation rate (annually 1600-1800 mm in the northeastern part of the study regions compared to rainfall values of 350 mm, see online evaporation statistics http://www.bom.gov.au/watl/evaporation/) makes it hard for surface water to be-

come groundwater. Only when there is sufficiently long-lasting rainfall in mountainous regions (e.g., May to August 40-80 mm, see, Fig 6a), does the surface water recharge groundwater. According to Fig 6b, groundwater in the mountainous regions only shows recharge to some extent during July and August (possibly, May and June are replenishing surface water first, e.g., producing a lag). In central mountainous regions of SWWA, *Kinal and Stoneman* (2012) report a phenomenon that surface water and groundwater are disconnected in dry seasons due to low rainfall level. Besides the three reasons above, groundwater depth, e.g., 10-30 m in central mountainous region could also be a contributing factor as to why the surface water does not reach groundwater, considering generally the low infiltration about mountainous granite or basalt rocks.

A further implication of this scenario is that when El Niño cause low levels of rainfall, the coastal regions and their recharge are affected due to the high correlation between rainfall and groundwater across the western coastline of SWWA (also see, e.g., *Holbrook et al.* 2009). During global teleconnection episodes, recharge in the mountainous regions may be completely unrelated to rainfall for the whole year due to insufficient rainfall caused by ENSO.

In terms of recharge/discharge speed, the coastal regions are generally faster than the mountainous regions because of different geological conditions, e.g., sandy soil in coastal regions are more easily penetrable by rainfall compared to granite rocks in the mountainous areas. Furthermore, a significant proportion of rainfall in mountainous regions becomes surface water that drains to coastal regions, producing an even faster recharge time in coastal areas near mountain regions (monthly recharge over 0.2 m). In the western coastal regions, the Gnangara groundwater system and Blackwood Plateau have a similar behaviour, where the recharge/discharge speed is slower than other regions such as region south of Perth (mostly less than 0.2 m per month) possibly due to different geological and topographic conditions.

4.2.3. Groundwater availability patterns

Based on the elevation profile of SWWA, the general groundwater flow direction should be from the east (higher elevation mountainous regions) to the west (lower elevation coastal regions of Perth basin), and finally into the Indian Ocean. However, there is a clear geographical boundary along the Darling Scarp that appears to lead to different groundwater behaviours on both sides (Fig 6c). This difference may in part be associated with rainfall since the difference in rainfall on either side of the scarp can reach 60-80 mm/month during rainy seasons. An average of 200 m difference in elevation exists across the scarp, as mentioned in Section 2, and geologically, the Darling Scarp and Darling fault's positions overlap with each other, which could be a natural barrier that blocks groundwater flow from the eastern mountainous regions to the coastal plain. This potential effect may need a detailed hydrogeological study that is beyond the scope of the current study. In addition, this boundary to the north appears to curve into mountain regions, departing from obvious landscape features, which may be biased due to sparse distribution of boreholes, and thus, is likely an artifact of the spatial interpolation (see, data density and coverage in Fig 8a).

The coastal regions from south of Perth to Busselton experience the lowest groundwater levels from April to June, and the highest groundwater levels from October to December (Fig 6c) in a year. The Gnangara groundwater system region, Blackwood Plateau, and central eastern side of the Darling Scarp appear to have similar groundwater behaviour, with groundwater levels from January to March being above average and from May to July, they are below average (Fig 6c). There are approximately 7-8 months in these three regions that groundwater level discharges from the level of highest peak to the lowest level. For these three regions, the Gnangara groundwater system is profoundly affected by human abstraction (*Awange*, 2012; *Skurray et al.*, 2012; *Awange and Kiema*, 2013; *Department of Water*, 2015; *Awange*, 2018; *Awange and Kiema*, 2019). Groundwater levels of the central eastern side of the Darling Scarp mostly correlate to the dams' water levels, e.g., the levels in Perth from 2012-2015 are mostly below average during April to August (see online: https://www.watercorporation.com.au/

water-supply/rainfall-and-dams/dam-levels) and this mirrors the results in Fig 6b. On the Blackwood Plateau, it is most likely that the groundwater is affected by geologic and topographic features, considering that it is surrounded by the Busselton and Darling faults (*CSIRO*, 2009), as well as three scarps (see Fig 7c, Whicher, Darling and Barlee Scarps).

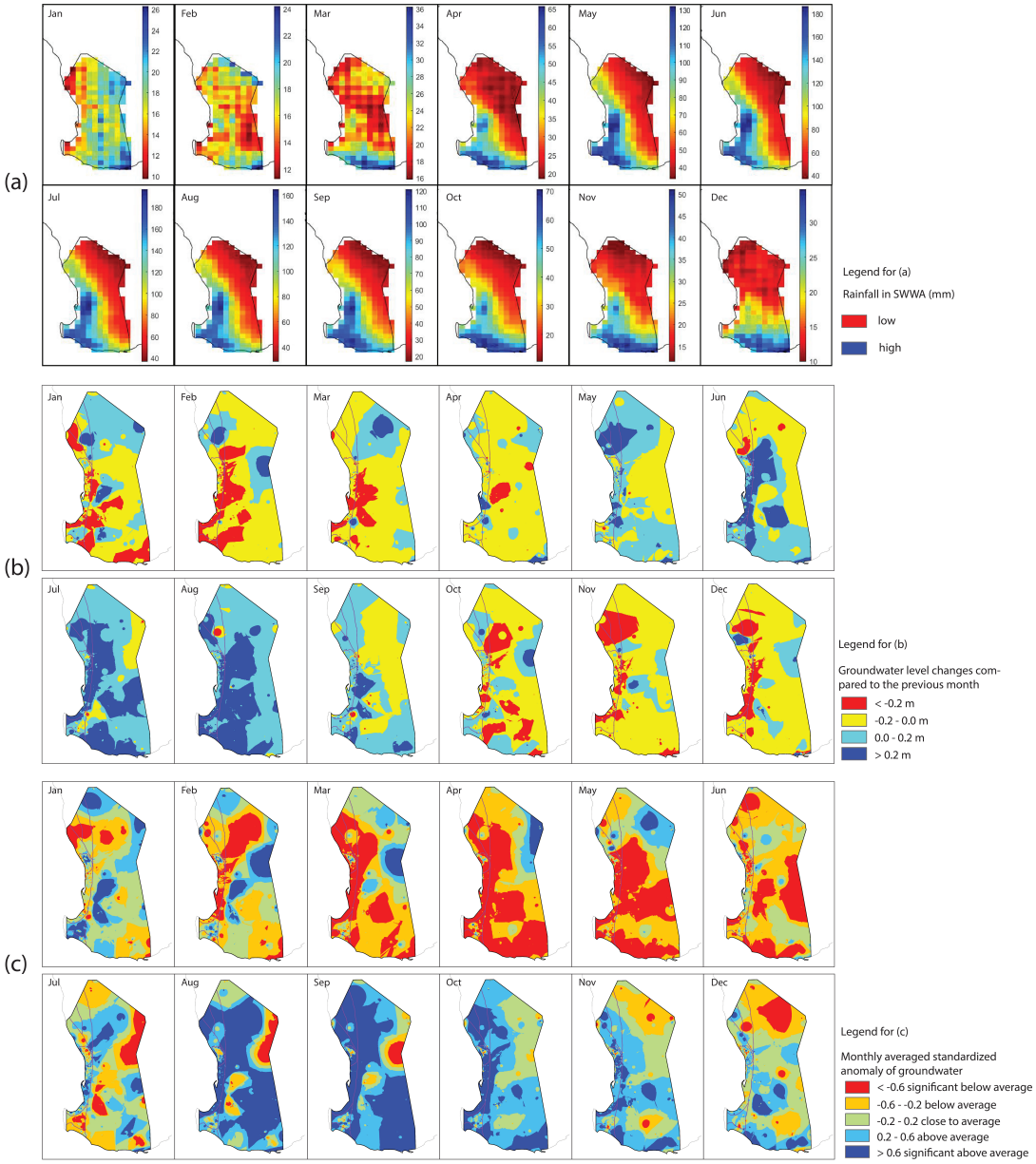

Figure 6: Monthly averaged spatial patterns of rainfall and standardized groundwater anomalies; (a) monthly averaged rainfall patterns (mm), (b) monthly averaged groundwater level changes compared to those of the previous month, and (c), monthly averaged standardized anomalies of groundwater. The Darling and Gingin Scarps appear to be barriers that divide rainfall between coastal and inland areas during the rainy season. The recharge/discharge show consistency along the western coastline in panel (b). Groundwater behaviours also appear different on either sides of the Darling and Gingin Scarps. North of Perth and Blackwood Plateau have similar groundwater patterns in panel (c). South coastal region and south of Perth requires at least 65-70 mm/month and 60 mm/month rainfall, respectively, to influence groundwater recharge according to postulations made based on the figures above.

4.3. Anthropogenic hotspots

Anthropogenic hotspots are identified as the boreholes with monthly groundwater level changes above 7 meters (as determined in Section 3.2.4), due to the likelihood of such a large change being below 1% in the overall study region. The frequency of these level changes is calculated according to each borehole's records, and the results presented in Fig 7. The identified anthropogenic hotspots occur mainly in the region north of Perth (the chance of groundwater level change above 7 m is around 18 to 55% for every month; see Fig 7), where the Gnangara groundwater system is located. This is to be expected since the Gnangara groundwater system contributes 50-60% of groundwater use in SWWA (*Skurray et al.*, 2012; *Department of Water*, 2015). Other remaining hotspots (chance below 18% per month) are the region south of Perth, close to dams (e.g., North Dandalup, Wellington, Shannon Dams), or close to mines (e.g., Collie mine), all of which are impacted by human activities.

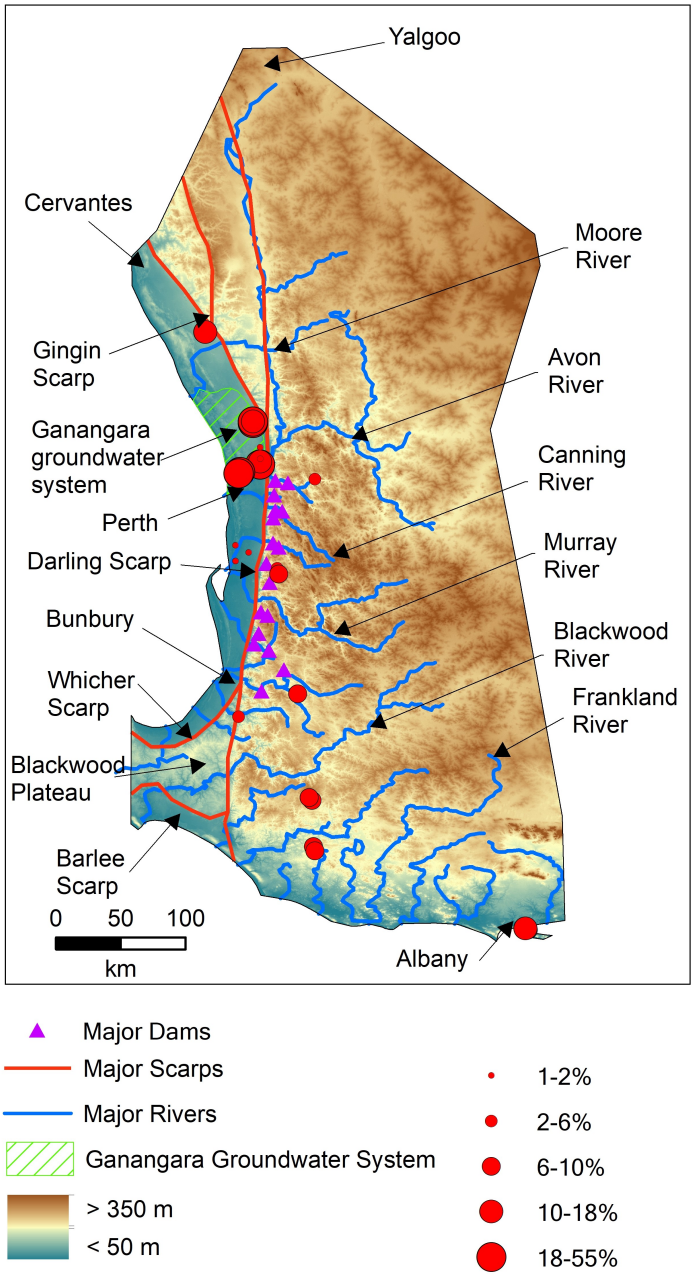

Figure 7: Anthropogenic hotspot locations in SWWA. Most of high chance hotspots (the chance of groundwater level change above 7 m is around 18 to 55% for every month) occur in Gnangara groundwater system, others are closed to dams or mines.

4.4. Spatial-temporal biases

Results presented in Sections 4.1 and 4.2 are likely to contain both spatial and temporal biases. According to Figs 1b and 8a, most data in terms of high spatial density and

long temporal coverage are located in the regions of north and south of Perth. Therefore, the long-term temporal analysis in Section 4.1 is more likely to represent groundwater behaviour in those regions. For the spatial-temporal interpolation results in Section 4.2, both IDW and Kriging methods show a significant difference in low density and short-term coverage areas of data (see the grey colour regions in Fig 8a), although results between them in others areas are statistically similar. Seven study regions (Fig 8b) are established according to their borehole density, rainfall, terrain characteristics, and groundwater systems, in order to discuss their spatial biases. Future studies will rigorously treat the problem of temporal biases.

Figure 9 shows the monthly anomalies of groundwater and rainfall for each study region indicated in Fig 8b, whose major findings are summarized in Table 1. In the previous Sections 4.1 and 4.2, groundwater was found to possess a good correlation with rainfall except in the mountainous regions (e.g., A and G in Fig 8b) of the study area. Therefore, no further consideration of the relationships between annual cycle variations of rainfall and groundwater is undertaken. The North mountainous region (A in Figs 8b and 9a) firstly appears to have more inter-seasonal rainfall variations (e.g. annual cycles change considerable from year to year) than other regions. On close examination, however, it is relatively low in magnitude, ranging from 10-45 mm (Fig 6a). In addition, the onset of the rainfall peak in the region as well as in North Perth region (B in Figs 8b and 9b) is earlier (May-July) than other regions (July - August). Groundwater in region A only weakly responds to rainfall variations except in the major rainy seasons. This weak response may be due to small rainfall amounts, terrain effects, high evaporation and/or groundwater depths (e.g., *Crissa and Davissonb* 1996; *Kinal and Stoneman* 2012). As already mentioned in Section 4.2.2, rather than becoming groundwater, the small amount of rainfall during dry periods in mountainous regions tend to evaporated or flow away because of terrain and geological effects (e.g., *Crissa and Davissonb* 1996). Additionally, groundwater levels do not appear to decline, although, there is considerable uncertainty due to the short-term data coverage and sparse borehole distribution.

Regions B and C (Figs 9b and 9c) are found where groundwater has major decline

after 2000, mostly attributed to human abstraction, see previous discussions in Sections 4.1.2 and 4.3. In the Central mountainous region (D in Figs 8b and 9d), which is adjacent to regions B and C, containing many dams located along the eastern side of the Darling Scarp, groundwater level variations mainly associate with dam levels, e.g., during the "Millennium drought", groundwater levels dropped significantly during the dry period 2002-2007, which agrees with dam level variations (see also the previous discussion in Section 4.2.3). For the Bunbury region (E in Figs 8b and 9e), the data are temporally discontinued but all show the same regular groundwater variation patterns. The Blackwood Plateau (F in Figs 8b and 9f) only has few years of consecutive data, with the results appearing to be affected by spatial bias (e.g., amplitudes are large for only a small number of boreholes, but small for a large number of boreholes). This possibly indicates high spatial variability of groundwater in this region. South mountainous region (G in Figs 8b and 9g) shows some similarities to the North mountainous region, in that groundwater levels do not appear to be strongly affected by rainfall except after long-lasting heavy rainfall. However, this region has lower evaporation rates and higher rainfall values compared to Region A, thus, rainfall and groundwater have stronger links. In addition, 4 boreholes showing an apparent anomalous level of -5 meters in 1995 are located in close proximity to a playground in Donnybrook (a small town in South mountainous region G), most likely are affected by anthropogenic impacts.

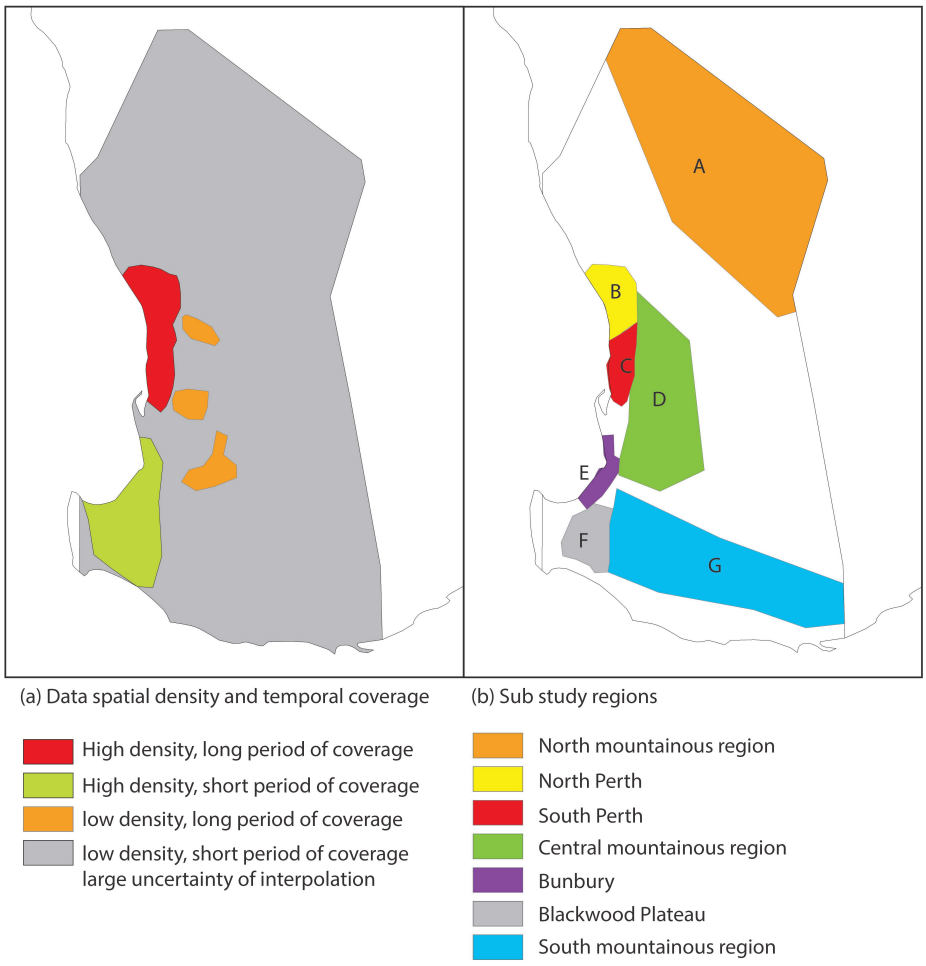

Figure 8: (a) spatial distribution of data density and temporal coverage where the gray regions indicate low reliability of interpolation results, and (b), sub study regions selected for bias discussions.

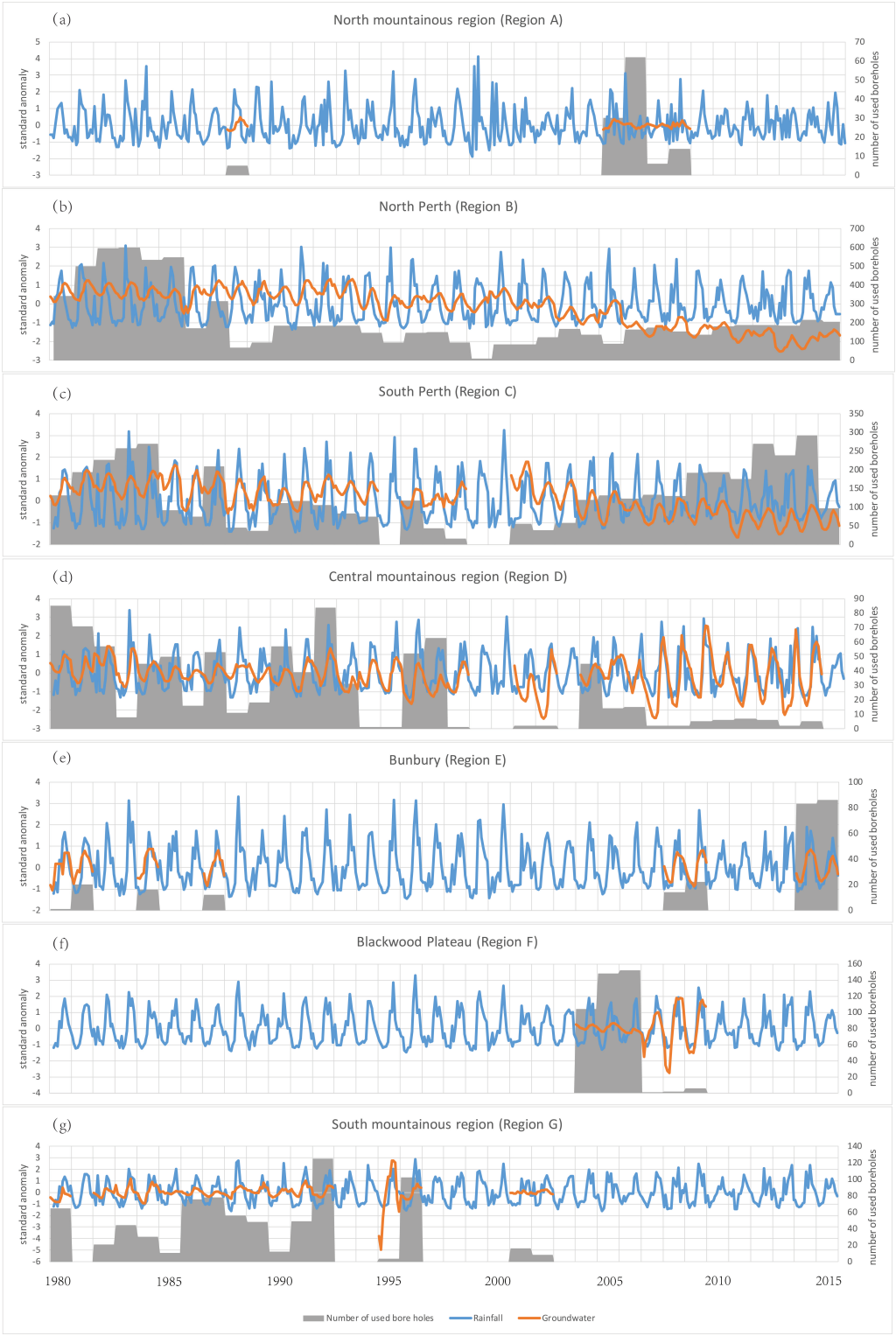

Figure 9: Comparison of monthly anomalies between groundwater and rainfall for each sub study region presented in Fig 8b. Rainfall patterns in most of the regions are similar, while the onset of the rainfall peaks in regions A and B are earlier (May - July) compared to other regions (July - August). The mountainous regions A and G only correlates to rainfall in rainy season. Major groundwater decline occurs in north and south of Perth (regions B and C). Blackwood Plateau (region F)'s groundwater varies spatially. Although Bunbury (region E) has insufficient data, it shows similar groundwater variations over the evaluated years.

Table 1: Summary of the major findings for each sub study region of Fig 8b in relation to Fig 9.

Region	Major findings
A (North mountainous region)	- Variable seasonal rainfall of small amounts, groundwater does not follow rainfall except during rainy season. - Rainfall peak occurs earlier compared to other regions (May-July vs. July - August). - Results could be biased due to only 5 years' data with very sparse borehole distribution
B (North Perth)	- This is an urban and major groundwater contribution area (Gnangara groundwater system). - Groundwater decline occurring after 2000 is caused by human abstraction (major) and continuous low rainfall (minor). - Groundwater in this region has 1-2 month(s)' lag with rainfall. Rainfall peaks are earlier compared to other regions (May-July vs. July - August). - Recharge speed is slower than other western coastal regions in SWWA.
C (South Perth)	- This is an urban area and groundwater decline occurring after 2000 is caused by human abstraction (major) and continuous low rainfall (minor). - 60 mm monthly rainfall is postulated as the threshold needed to recharge groundwater.
D (Central mountainous region)	- Groundwater follows rainfall and matches dam level variations, could be affected by terrain (Darling Scarp), geological (Darling fault and rock types), and anthropogenic effects (dam).
E (Bunbury)	- Temporally discontinuous groundwater data coverage, however shows uniform temporal groundwater variation patterns. Groundwater is stable.
F (Blackwood)	- High spatial variability of groundwater in this region, could be affected by Whicher, Barlee and Darling Scarps. - Similar to region B, the groundwater in this region has 1-2 month(s)' lag with rainfall.
G (South mountainous regions)	- Similar to Region A, but groundwater appears to have slightly better response to rainfall, particular during rainy seasons.

5. Conclusion

South-West Western Australia (SWWA) is a region that heavily relies on groundwater for agricultural and domestic water use, especially during dry periods. However, the decline of groundwater since 2000 and the lack of spatio-temporal variability studies undertaken in this region impose challenges on groundwater management. This contribution employed a suit of statistical tools such as Man-Kendall test, cross-correlation, cross-validation, Kolmogorov-Smirnov test, and regression analysis, to investigate and provide a more in-depth understanding the spatio-temporal variations of groundwater in SWWA for the period 1980-2015, and identified its potential interconnections to climate variability/change and anthropogenic impacts. The major findings corresponding to objectives can be summarized as:

1. For variability of groundwater in SWWA, the north and south of Perth were the main regions that experienced groundwater decline since 2000, with a decreasing rate of 13 mm/month (or 156 mm/year). Other regions' groundwater levels appeared to be stable.

2. For groundwater availability, the high and low level of groundwater in SWWA are from July to January (high) and February to June (low). As for recharge/discharge, the western coastal regions exhibit a faster recharge speed than eastern mountainous regions. Among western coastal regions, north of Perth (Gnangara groundwater system) and Blackwood Plateau have slower groundwater recharge/discharge speed than other areas.

3. For spatial pattern of variations and recharge/discharge, groundwater levels over the northeastern mountainous regions were generally not affected by rainfall during dry periods, due to the fact that small amount of rainfall in the mountain regions tends to evaporated and flow away rather than become groundwater. The western coastline region's groundwater follows rainfall variations. In addition, most of SWWA region's groundwater have no lags between rainfall and groundwater. A postulated minimum threshold of rainfall to recharge groundwater for the region

south of Perth and southern coastline of SWWA is around 60 mm/month and 65-70 mm/month, respectively. North of Perth (Gnangara groundwater system) and Blackwood Plateau have 1-2 month(s)'s lag between rainfall and groundwater.

4. For climate variability/change impacts to groundwater, the overall patterns of spatio-temporal variability of rainfall were relative uniform over SWWA, with the major rainy season from May to September. No significant declining trend in rainfall was detected after 2000. However, average annual total rainfall for the period 2000-2015 decreased by 40 mm compared to the period of 1980-1999. The continuous low level of rainfall after 2000, however, may partly contribute to the decline of groundwater. In addition, when ENSO caused low level of rainfall, groundwater recharge in coastal regions was significantly affected.

5. In regards to anthropogenic hotspots identification and impacts on groundwater, most are identified in the regions north of Perth (Gnangara groundwater system), and south of Perth, as well as, close to dams and mines. Anthropogenic impacts such as human abstraction were the primary reasons for groundwater decline in these regions. Finally, different behaviours of groundwater on either side of the Darling Scarp were caused by other factors such as rainfall, terrain, geological faults, aquifers and dams. A detailed analysis and discussion of these factors, however, is outside the scope of this study and will be considered in future contributions.

Acknowledgment

Kexiang Hu is grateful for the CIPRS and Research Stipend Scholarship provided by Curtin University that is supporting his PhD studies. J.L. Awange would like to thank the financial support of the Alexander von Humboldt Foundation that supported his stay at Karlsruhe Institute of Technology. He is grateful to the good working atmosphere provided by his hosts Prof Hansjörg Kutterer and Prof Bernhard Heck. The authors would like to thank the following organizations for providing the data used in this study; the Australian Bureau of Meteorology (BoM), Princeton Climate Analytics (PCA) and

717 Earth System Research Laboratory. In addition, special thanks to Prof. Paul Tregoning
718 who provided valuable suggestions for this paper.

References

ABARES (2018), About my region - Western Australia, *Report*, Australia Government, Department of Agriculture and Water Resources, retrieved from http://www.agriculture.gov.au/abares/research-topics/aboutmyregion/wa. Data accessed: 3 March, 2019.

Agriculture and Food (2018), Western Australia's agriculture and food sector, *Report*, Australia Government, Department of Primary Industries and Regional Development, retrieved from https://www.agric.wa.gov.au/western-australias-agriculture-and-food-sector. Data accessed: 6 March, 2019.

Alexander, S. (2018), Population growth and the mining industry in western australia, *Blog*, ABS, retrieved from https://demogblog.blogspot.com/2018/06/population-growth-and-mining-industry.html. Data accessed: 1 July, 2019.

Ali, R., D. McFarlane, S. Varma, W. Dawes, I. Emelyanova, and G. Hodgson (2012), Potential climate change impacts on groundwater resources of south-western Austalia, *Journal of Hydrology*, *475*, 456–472, doi:10.1016/j.jhydrol.2012.04.043.

Alley, W. (2009), Encyclopedia of Inland Waters, *Reference Module in Earth System and Environmental Sciences*, pp. 684–690, doi:10.1016/B978-012370626-3.00015-6.

Anyah, R., E. Forootan, J. Awange, and M. Khaki (2018), Understanding linkages between global climate indices and terrestrial water storage changes over Africa using GRACE products, *Science of the Total Environment*, *635*, 1405–1416, doi:10.1016/j.scitotenv.2018.04.159.

Argent, R. (2016), Inland water: Groundwater resources, Australia state of the environment 2016, *Tech. rep.*, Australian Government Department of the Environment and Energy, Canberra, doi:10.4226/94/58b656cfc28d1.

Ashok, K., Z. Guan, and T. Yamagata (2003), Influence of the Indian Ocean Dipole

on the Australian winter rainfall, *Geophysical Research Letters*, *30*(15), CLM6, 1–4, doi:10.1029/2003GL017926.

Awange, J. (2012), *Environmental Monitoring using GNSS: Global Navigation Satellite Systems*, Springer-Verlag Berlin Heidelberg, doi:10.1007/978-3-540-88256-5.

Awange, J. (2018), *GNSS Environmental Sensing: Revolutionizing Environmental Monitoring*, Springer International Publishing, doi:10.1007/978-3-319-58418-8.

Awange, J., and J. Kiema (2013), *Environmental Geoinformatics: Monitoring and Management (Environmental Science and Engineering)*, Springer-Verlag Berlin Heidelberg, doi:10.1007/978-3-642-34085-7.

Awange, J., and J. Kiema (2019), *Environmental Geoinformatics: Extreme Hydro-Climatic and Food Security Challenges: Exploiting the Big Data*, Springer-Verlag Berlin Heidelberg, doi:10.1007/978-3-030-03017-9.

Awange, J., L. Ogalo, K. Bae, P. Were, P. Omondi, P. Omute, and M. Omullo (2008), Falling Lake Victoria water levels: Is climate a contributing facotr?, *Climate Change*, *89*, 281–297, doi:10.1007/s10584-008-9409-x.

Awange, J., M. Sharifi, O. Baur, W. Keller, W. Featherstone, and M. Khun (2010), GRACE hydrological monitoring of Australia: Current limitations and future prospects, *Journal of Spatial Science*, *54*(1), 23–26, doi:10.1080/14498596.2009.9635164.

Awange, J., K. Fleming, M. Kuhn, W. Featherstone, B. Heck, and I. Anjasmara (2011), On the suitability of the 4 degrees x 4 degrees GRACE mascon solutions for remote sensing Australian hydrology, *Remote Sensing of Environment*, *115*(3), 684–690, doi:10.1016/j.rse.2010.11.014.

Awange, J., F. Mpelasoka, and R. Goncalves (2016), When every drop counts: Analysis of Droughts in Brazil for the 1901-2013 period, *Science of The Total Environment*, *566-567*, 1472–1488, doi:10.1016/j.scitotenv.2016.06.031.

771 Awange, J., K. Hu, and M. Khaki (2019), The newly merged satellite remotely sensed,
772 gauge and reanalysis-based Multi-Source Weighted-Ensemble Precipitation: Evalua-
773 tion over Australia and Africa (1981-2016), *Science of the Total Environment*, *670*,
774 448–465, doi:10.1016/j.scitotenv.2019.03.148.

775 Barron, O., R. Crosbie, S. Charles, W. Dawes, R. Ali, W. Evans, R. Cresswell, D. Pollock,
776 G. Hodgson, D. Currie, F. Mpelasoka, T. Pickett, S. Aryal, M. Donn, and B. Wurcker
777 (2011), Climate change impact on groundwater resources in Australia, *Summary report*,
778 CSIRO Water for a Healthy Country Flagship, Australia, retrieved from: https://
779 publications.csiro.au/rpr/download?pid=csiro:EP121194&dsid=DS1. Data ac-
780 cessed: 10 March, 2019.

781 Beck, H., A. van Dijk, V. Levizzani, J. Schellekens, D. Miralles, and A. d. R. B. Martens
782 (2017a), MSWEP: 3-hourly 0.25° global gridded precipitation (1979-2015) by merging
783 gauge, satellite, and reanalysis data, *Hydrology and Earth System Sciences*, *21,*, 589–
784 615, doi:10.5194/hess-21–589-2017.

785 Beck, H., N. Vergopolan, M. Pan, V. Levizzani, A. van Dijk, G. Weedon, L. Brocca,
786 F. Pappenberger, G. Huffman, and E. Wood (2017b), Global-scale evaluation of 22
787 precipitation datasets using gauge observations and hydrological modeling, *Hydrology*
788 *and Earth System Sciences*, *21*, 6201–6217, doi:10.5194/hess-21-6201-2017.

789 Bhanja, S., M. Rodell, B. Li, D. Saha, and A. Mukherjee (2016), Spatio-temporal
790 variability of groundwater storage in India, *Journal of Hydrology*, *544*, 428–437,
791 doi:10.1016/j.jhydrol.2016.11.052.

792 Cai, W., P. van Rensch, and T. Cowan (2011), Teleconnection Pathways of ENSO and
793 the IOD and the Mechanisms for Impacts on Australian Rainfall, *Journal of climate*,
794 *24*, 3910–3923, doi:10.1175/2011JCLI4129.1.

795 Cai, W., T. Purich, A.and Cowan, P. van Rensch, and E. Weller (2014), Did climate
796 change–induced rainfall trends contribute to the Australian Millennium Drought?,
797 *Journal of Climate*, *27*(9), 3145–3168, doi:10.1175/JCLI-D-13-00322.1.

798 Chen, J., C. Wilson, B. Tapley, B. Scanlon, and A. Güntner (2016), Long-term groundwa-
799 ter storage change in Victoria, Australia from satellite gravity and in situ observations,
800 *Global and Planetary Change*, *139*, 56–65, doi:10.1016/j.gloplacha.2016.01.002.

801 Crissa, R., and M. Davissonb (1996), Isotopic imaging of surface water/groundwater
802 interactions, Sacramento Valley, California, *Journal of Hydrology*, *178*(1-4), 205–222,
803 doi:10.1016/0022-1694(96)83733-4.

804 CSIRO (2009), Groundwater yields in south-west Western Australia. A report to the
805 Australian Government from the CSIRO South-West Western Australia Sustainable
806 Yields Project, *Tech. rep.*, CSIRO Water for a Healthy Country Flagship, Australia,
807 retrieved from: https://publications.csiro.au/rpr/download?pid=legacy:726&
808 dsid=DS1. Data accessed: 6 March, 2019.

809 Dawes, W., R. Ali, S. Varma, I. Emelyanova, G. Hodgson, and D. McFarlane (2012),
810 Modelling the effects of climate and land cover change on groundwater recharge in
811 south-west Western Australia, *Hydrology and Earth System Sciences*, *16*, 2709–2722,
812 doi:10.5194/hess-16-2709-2012.

813 Departement of Water (2009), SouthWest - groundwater areas allocation plan,
814 *Water report 21*, Government of Western Australia, Department of Wa-
815 ter, retrieved from https://www.water.wa.gov.au/__data/assets/pdf_file/
816 0013/1822/86107.pdf. Data accessed: 6 March, 2019.

817 Department of Water (2007), State Water Plan 2007, *Report*, Department of Water,
818 Government of Western Australia, retrieved from https://www.water.wa.gov.au/__
819 data/assets/pdf_file/0015/4524/74923.pdf. Data accessed: 10 March, 2019.

820 Department of Water (2015), Environmental management of groundwater from the
821 Gnangara Mound, *Triennial compliance report to the office of the environmental*
822 *protection authority*, Government of Western Australia, Department of Water, re-
823 trieved from http://www.water.wa.gov.au/__data/assets/pdf_file/0006/9591/
824 Gnangara-Compliance-Report.pdf. Data accessed: 3 March, 2019.

Eamus, D. (2015), Decling groundwater is a big problem for Australia, *ABC NEWS*, environmental Sciences at the University of Technology, retrieved from: https://www.abc.net.au/news/2015-06-18/eamus-declining-groundwater-is-a-big-problem-for-australia/6556586. Data accessed: 10 March, 2019.

Featherstone, W., M. Filmer, N. Pena, L. Morgan, and A. Schenk (2012), Anthropogenic land subsidence in the Perth Basin: Challenges for its retrospective geodetic detection, *Journal of the Royal Society of Western Australia*, *95*(1), 53–62, doi:http://hdl.handle.net/20.500.11937/14837.

Fleming, K., and J. Awange (2013), Comparing the version 7 TRMM 3B43 monthly precipitation product with the TRMM 3B43 version 6/6A and Bureau of Meteorology datasets for Australia, *Australian Meteorological and Oceanographic Journal*, *63*, 421–426, doi:10.22499/2.6303.007.

Fleming, K., J. Awange, M. Kuhn, and W. Featherstone (2011), Evaluating the TRMM 3B43 monthly precipitation product using gridded raingauge data over Australia, *Australian Meteorological and Oceanographic Journal*, *61*, 171–184, retrieved from: https://espace.curtin.edu.au/bitstream/handle/20.500.11937/23560/169513_169513.pdf?sequence=2. Data accessed: 3 March, 2019.

Forootan, E., Khandu, J. Awange, M. Schumacher, R. Anyah, A. van Dijk, and J. Kusche (2016), Quantifying the impacts of ENSO and IOD on rain gauge and remotely sensed precipitation products over Australia, *Remote Sensing of Environment*, *172*, 50–66, doi:10.1016/j.rse.2015.10.027.

Han, D., M. Currell, G. Cao, and B. Hall (2017), Alterations to groundwater recharge due to anthropogenic landscape change, *Jouranl of Hydrology*, *554*, 545–557, doi:10.1016/j.jhydrol.2017.09.018.

Heberger, M. (2011), *Australia's Millennium Drought: Impacts and Responses*, pp. 97–125, Island Press/Center for Resource Economics, Washington, DC, doi:10.5822/978-1-59726-228-6_5.

853 Hill, M., G. Donald, M. Hyder, and R. Smith (2004), Estimation of pasture growth rate
854 in the south west of Western Australia from AVHRR NDVI and climate data, *Remote*
855 *Sensing of Environment*, *93*(4), 528–545, doi:10.1016/j.res.2004.08.006.

856 Holbrook, N., J. Davidson, M. Feng, A. Hobday, J. Lough, S. McGregor, and J. Ris-
857 bey (2009), El Niño-Southern Oscillation, *In a marine climate chnage impacts and*
858 *adaptation report card for australia 2009*, NCCARF, publication 05/09, ISBN 978-1-
859 921609-03-09.

860 Hu, K., J. Awange, Khandu, E. Forootan, R. Goncalves, and K. Fleming (2017),
861 Hydrogeological characterisation of groundwater over Brazil using remotely sensed
862 and model products, *Science of The Total Environment*, *599-600*, 372–386,
863 doi:10.1016/j.scitotenv.2017.04.188.

864 Hughes, J., K. Petrone, and R. Silberstein (2012), Drought, groundwater storage and
865 stream flow decline in southwestern Australia, *Geophysical Research Letters*, *39*(3),
866 L03,408, doi:10.1029/2011GL050797.

867 Jenks, G. (1967), The Data Model Concept in Statistical Mapping, *International Year-*
868 *book of Cartography*, *7*, 186–190.

869 Kinal, J., and G. Stoneman (2012), Disconnection of groundwater from surface water
870 causes a fundamental change in hydrology in a forested catchment in south-western
871 Australia, *Journal of Hydrology*, *472-473*, 14–24, doi:10.1016/j.jhydrol.2012.09.013.

872 Knapp, C., and G. Carter (1976), The generalized correlation method for estimation
873 of time delay, *IEEE Transactions on Acoustics, Speech and Signal Processing*, *24*(4),
874 320–327, doi:10.1109/TASSP.1976.1162830.

875 Leblance, M., P. Tregoning, G. Ramillien, S. Tweed, and A. Fakes (2009), Basin-scale,
876 integrated observations of the early 21st century multiyear drought in southeast Aus-
877 tralia, *Water Resources Research*, *45*(4), W04,408, doi:10.1029/2008WR007333.

878 Li, J., S. Xie, E. Cook, M. Morales, D. Christie, N. Johnson, F. Chen, R. Arrigo,

879 A. Fowler, X. Gou, and K. Fang (2013), El Niño modulations over the past seven
880 centuries, *Nature Climate Change*, *3*, 822–826, doi:10.1038/nclimate1936.

881 Mann, H. B. (1945), Noparametric tests against trend, *Econometrica*, *13*, 163–171.

882 Massey, F. (1951), The Kolmogorov-Smirnov Test for Goodness of Fit, *Journal of the*
883 *American Statistical Association*, *46*(253).

884 Nicholls, N., W. Drosdowsky, and B. Lavery (1997), Australian rainfall variability and
885 change, *Weather*, *52*, 66–72, doi:10.1002/j.1477-8696.1997.tb06274.x.

886 Niedzielski, T. (2014), Chapter Two - EI Niño/Southern Oscilation and Se-
887 leced Environmental Consequences, *Advances in Geophysics*, *55*, 77–122,
888 doi:10.1016/bs.agph.2014.08.002.

889 Nikroo, L., M. Zare, A. Sepaskhah, and S. Shamsi (2008), Groundwater depth and ele-
890 vation interpolation by kriging methods in Mohr Basin of Fars province in Iran, *Envi-*
891 *ronment Monitoring Assessment*, *166*, 387–407, doi:10.1007/s10661-009-1010-x.

892 Oliver, M. A. (1990), Kriging: A Method of Interpolation for Geographical Information
893 Systems, *International Journal of Geographic Information Systems*, *4*, 313–332.

894 Philip, G. M., and D. F. Watson. (1982), A Precise Method for Determining Contoured
895 Surfaces, *Australian Petroleum Exploration Association Journal*, *22*, 205–212.

896 Population Australia (2018), Population of Western Australia 2019, *Popu-*
897 *lation report*, Australia Bureau of Statistics, Australian Government and
898 Tourism Western Australia, retrieved from `http://www.population.net.au/`
899 `population-of-western-australia/`. Data accessed: 3 March, 2019.

900 Rieser, D., M. Kuhn, R. Pail, I. Anjasmara, and J. Awange (2010), Relation between
901 GRACE-derived surface mass variations and precipitation over Australia, *Australian*
902 *Journal of Earth Sciences*, *57*(7), 887–900, doi:10.1080/08120099.2010.512645.

Robinson, T., and G. Metternicht (2006), Testing the performance of spatial interpolation techniques for mapping soil properties, *Computers and Electronics in Agriculture*, *50*, 97–108, doi:10.1016/j.compag.2005.07.003.

Saji, N., and T. Yamagata (2003), Possible impacts of Indian Ocean Dipole mode events on global climate, *Climate Research*, *25*(2), 151–169, retrieved from: https://www.int-res.com/abstracts/cr/v25/n2/p151-169/. Data accessed: 6 March, 2019.

Saleem, A., and J. L. Awange (2019), Coastline shift analysis in data deficient regions: Exploiting the high spatiotemporal resolution Sentinel-2 products, *Catena*, *179*, 6–19, doi:10.1016/j.catena.2019.03.023.

Skurray, J., E. Roberts, and D. Pannell (2012), Hydrological challenges to groundwater trading: Lessons from south-west Western Australia, *Journal of Hydrology*, (412-413), 256–268, doi:10.1016/j.jhydrol.2011.05.034.

Strassberg, G., B. Scanlon, and D. Chambers (2009), Evaluation of groundwater storage monitoring with the GRACE satellite: Case study of the High Plains aquifer, central United States, *Water Resources Research*, *45*(5), W05,410, doi:10.1029/2008WR006892.

Suh, J., P. Brown, and G. Birch (2003), Hydrogeochemical characteristics and importance of natural and anthropogenic influences on soil and groundwater in reclaimed land adjacent to Port Jackson, Sydney, Australia, *Marine and Freshwater Research*, *54*(6), 767–779, doi:10.1071/MF02075.

Sun, Y., S. Kang, F. Li, and L. Zhang (2009), Comparison of interpolation methods for depth to groundwater and its temporal and spatial variations in the Minqin oasis of northwest China, *Environmental Modelling and Software*, *24*, 1163–1170, doi:10.1016/j.envsoft.2009.03.009.

Taylor, R., B. Scanlon, P. Döll, M. Rodell, R. van Beek, Y. Wada, L. Longuevergne, M. Leblanc, J. Famiglietti, M. Edmunds, L. Konikow, T. Green, J. Chen, M. Taniguchi, M. Bierkens, A. MacDonald, Y. Fan, R. Maxwell, Y. Yechieli, J. Gurdak, D. Allen,

M. Shamsudduha, K. Hiscock, P. Yeh, I. Holman, and H. Treidel (2013), Groundwater and climate change, *Nature Climate Change*, *3*, 322–329, retrieved from: https://www.nature.com/articles/nclimate1744. Data accessed: 6 March, 2019.

Tregoning, P., S. McClusky, A. van Dijk, R. Crosbie, and J. Peña-Arancibia (2012), Assessment of GRACE satellites for groundwater estimation in Australia, *Waterlines report*, National Water Commission, Canberra, retrieved from: https://www.researchgate.net/publication/233757174. Data accessed: 3 March, 2019.

Tudhope, A., C. Chilcott, M. McCulloch, E. Cook, J. Chappell, R. Ellam, D. Lea, J. Lough, and G. Shimmield (2001), Variability in the EI Niño-Southern Oscillation Through a Glacial-Interglacial Cycle, *Science*, *291*(5508), 1511–1517, doi:10.1126/science.1057969.

Tweed, S., M. Leblanc, J. Webb, and M. Lubczynski (2007), Remote sensing and GIS for mapping groundwater recharge and discharge areas in salinity prone catchments, southeastern Australia, *Hydrogeology Journal*, *15*(1), 75–96, doi:10.1007/s10040-006-0129-x.

Wolter, K., and M. Timlin (1998), Measuring the strength of ENSO - how does 1997/98 rank?, *Weather*, *53*, 315–324, doi:10.1002/j.1477-8696.1998.tb06408.x.

Figure 1

Click here to download high resolution image

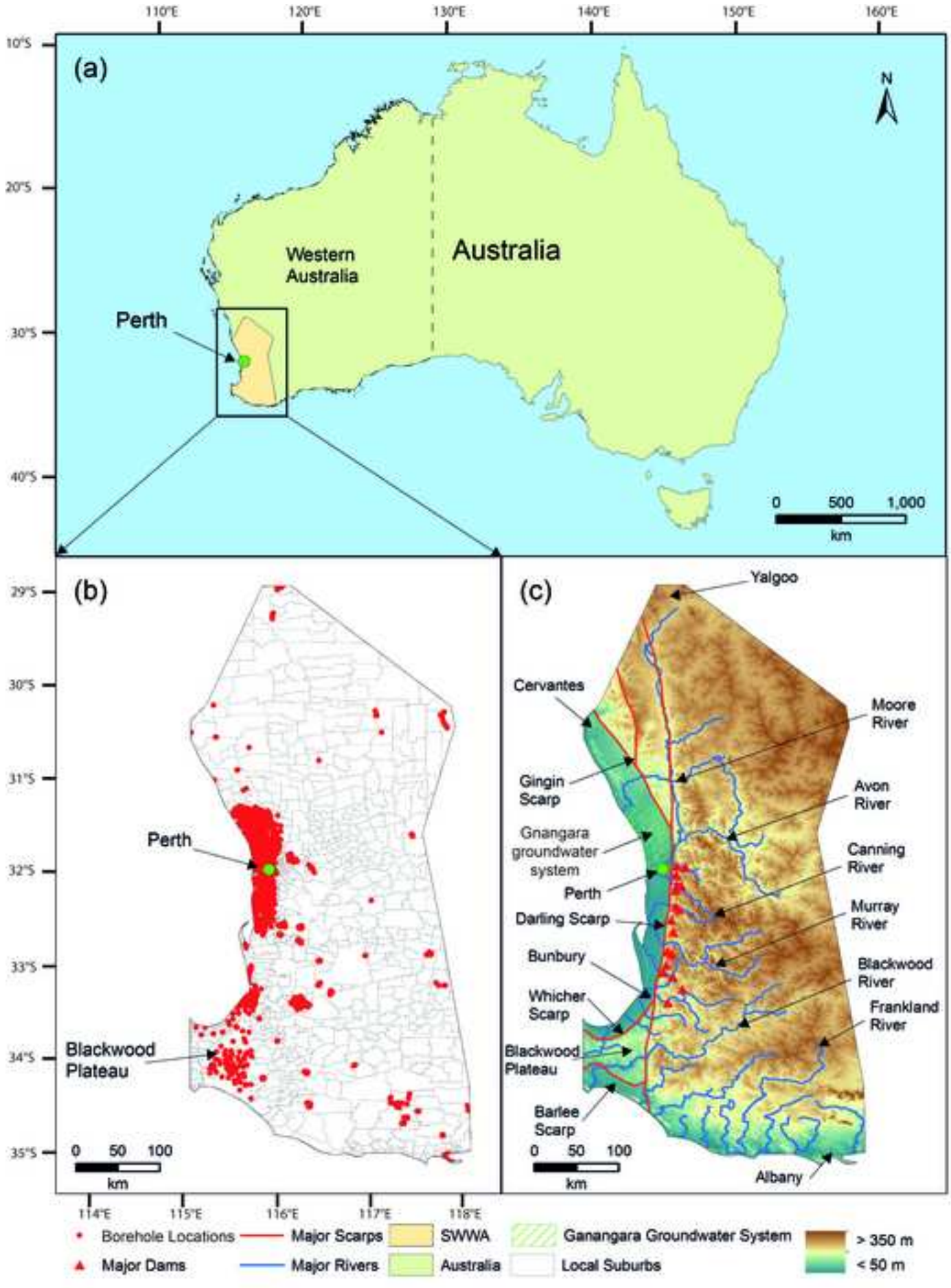

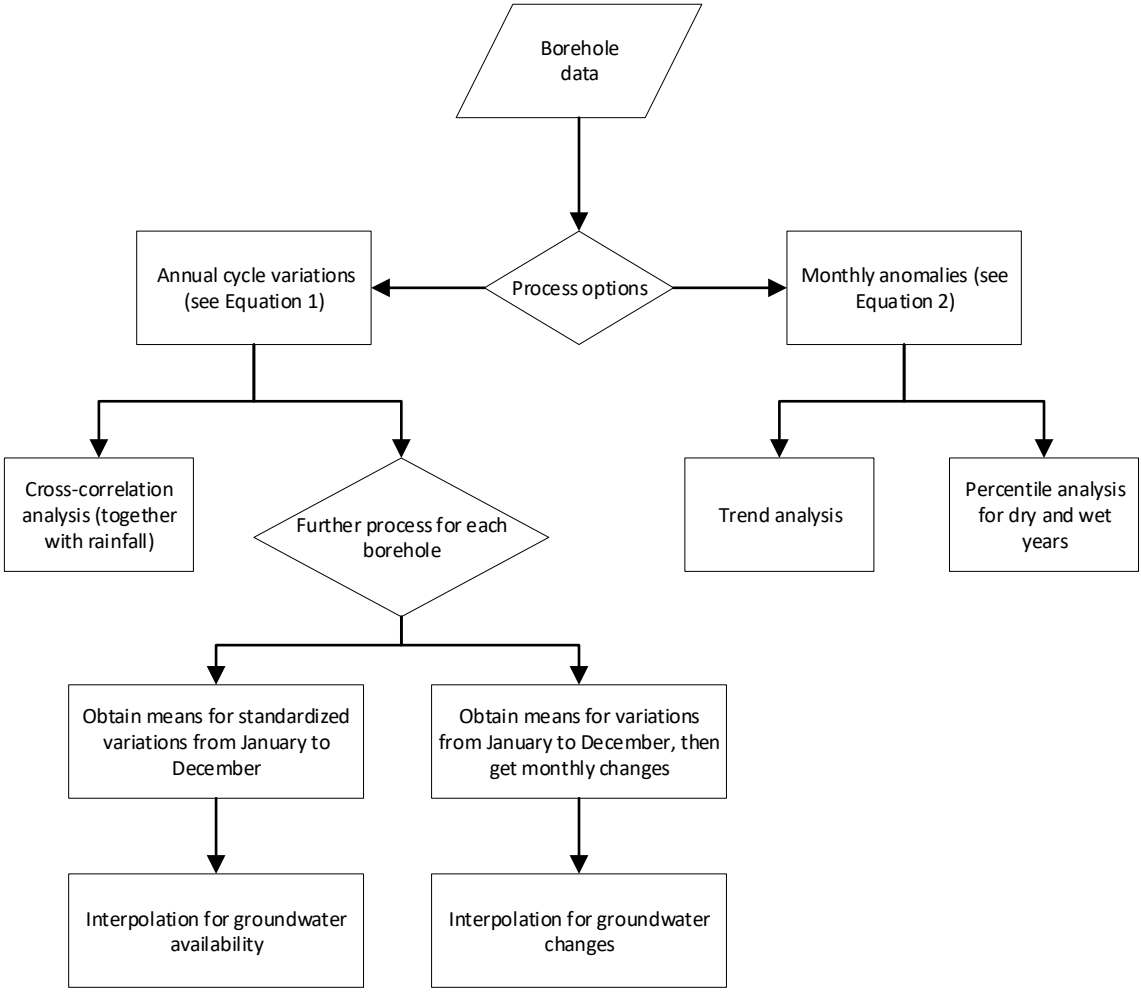
Borehole data
Process options
Annual cycle variations (see Equation 1)
Monthly anomalies (see Equation 2)
Cross-correlation analysis (together with rainfall)
Further process for each borehole
Trend analysis
Percentile analysis for dry and wet years
Obtain means for standardized variations from January to December
Obtain means for variations from January to December, then get monthly changes
Interpolation for groundwater availability
Interpolation for groundwater changes

Figure 3

Click here to download high resolution image

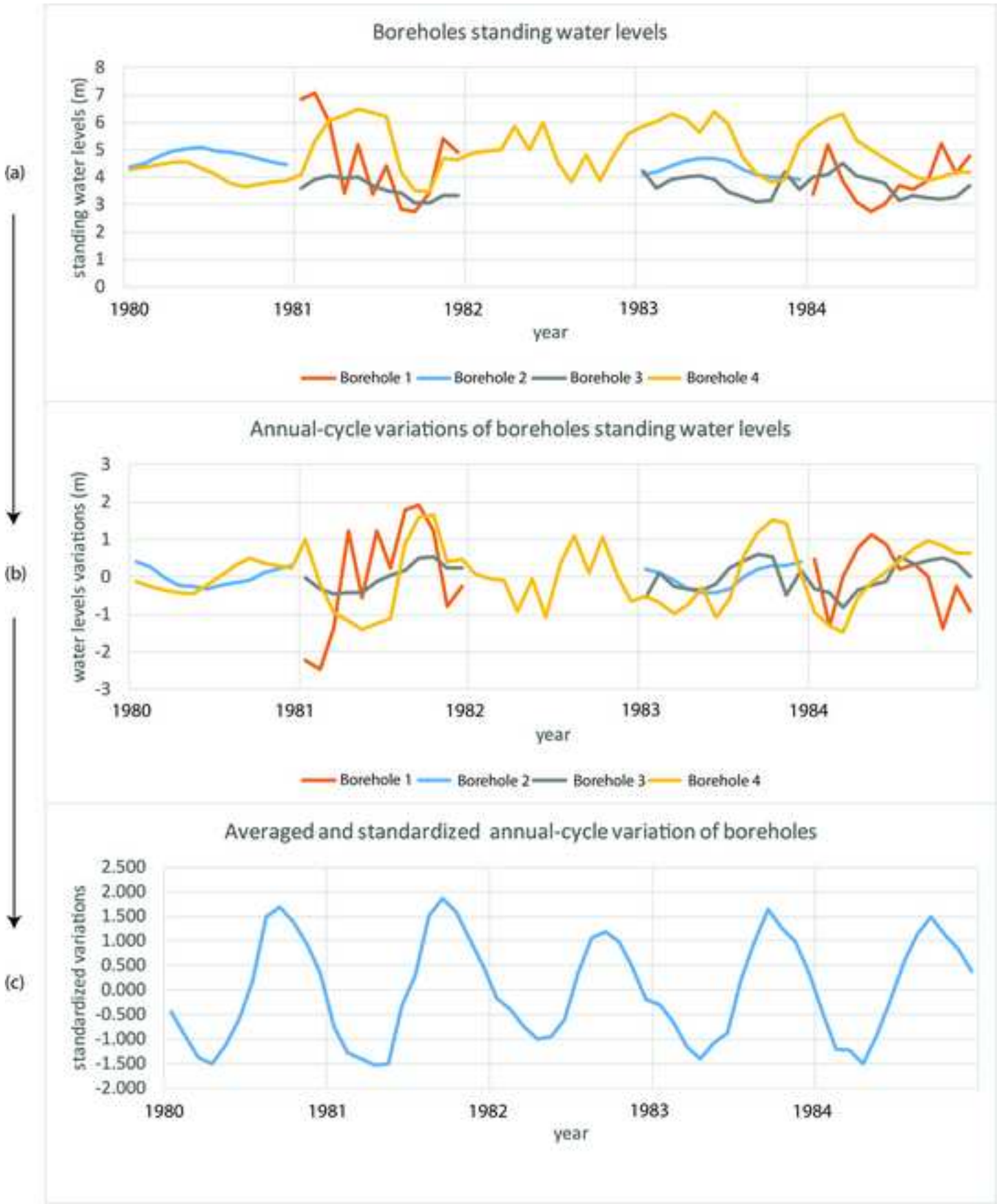

Figure 4

Click here to download high resolution image

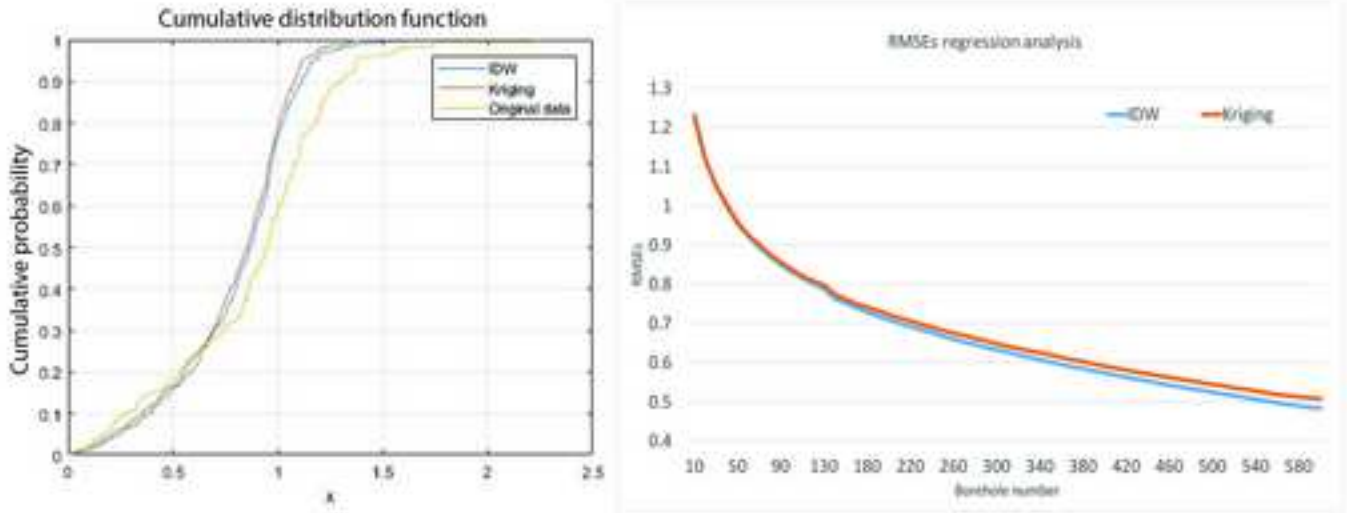

(a) K-S test cumulative distribution

(b) Regression analysis

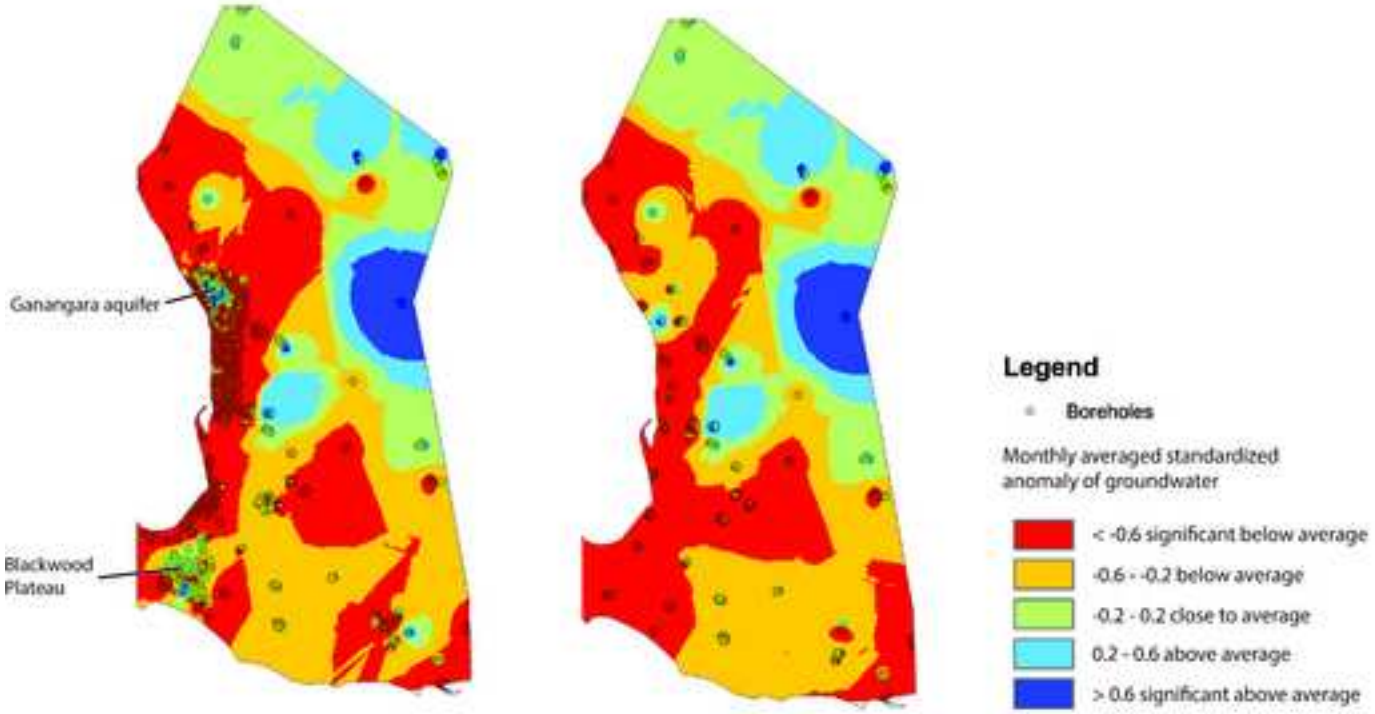

(c) Original IDW interpolation for March

(d) IDW interpolation with sparse boreholes for March

Figure 5

Click here to download high resolution image

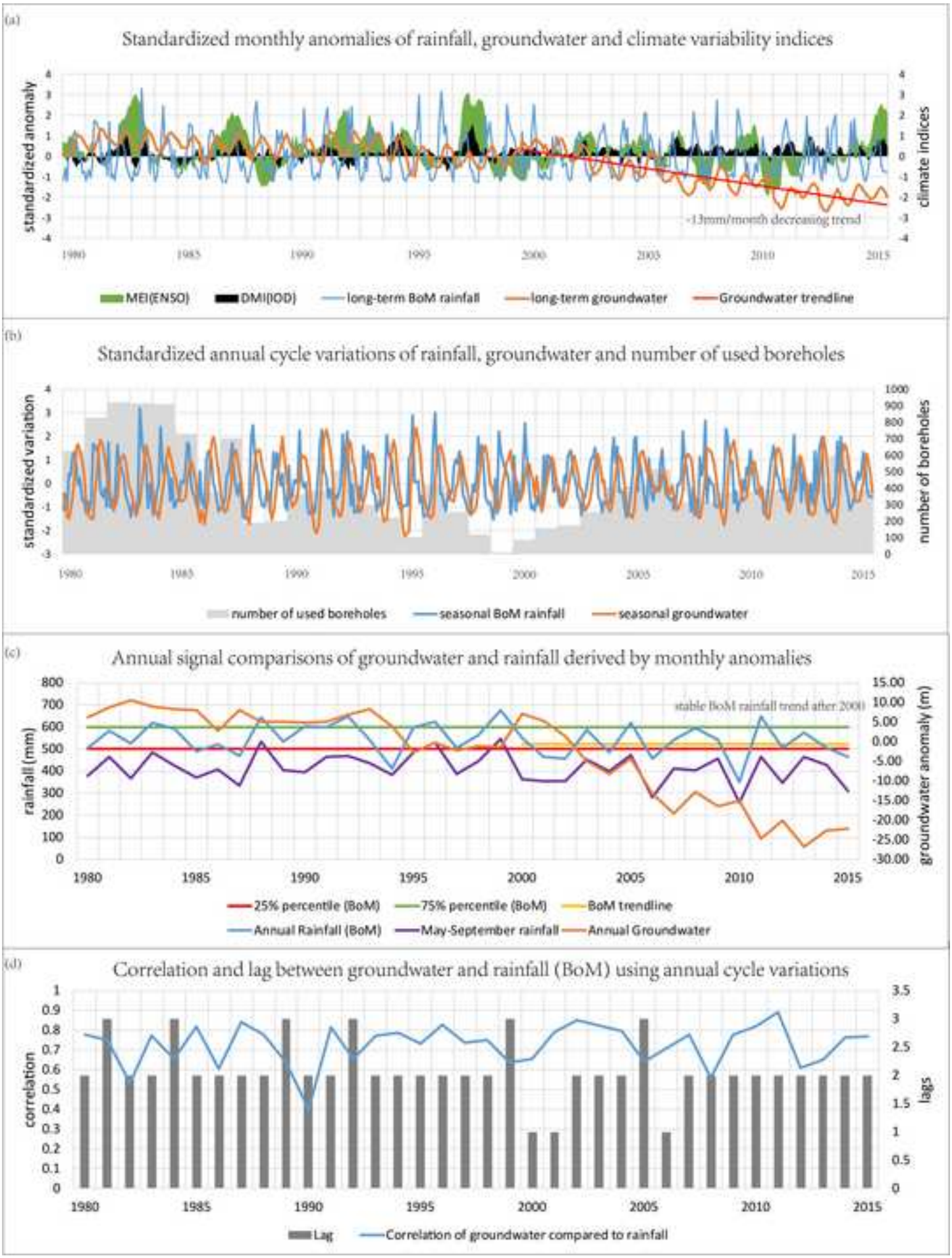

Figure 6

Click here to download high resolution image

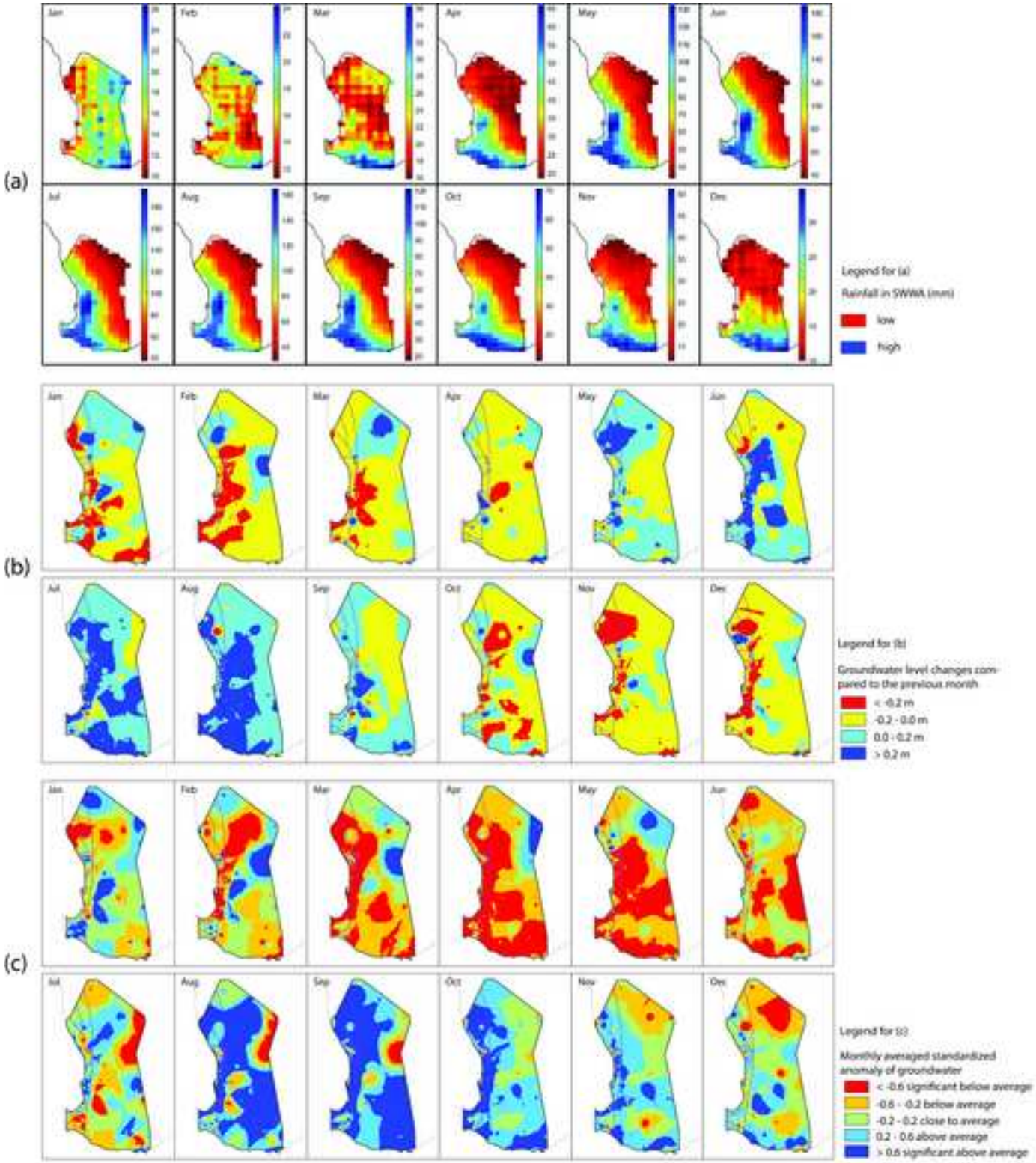

Figure 7

Click here to download high resolution image

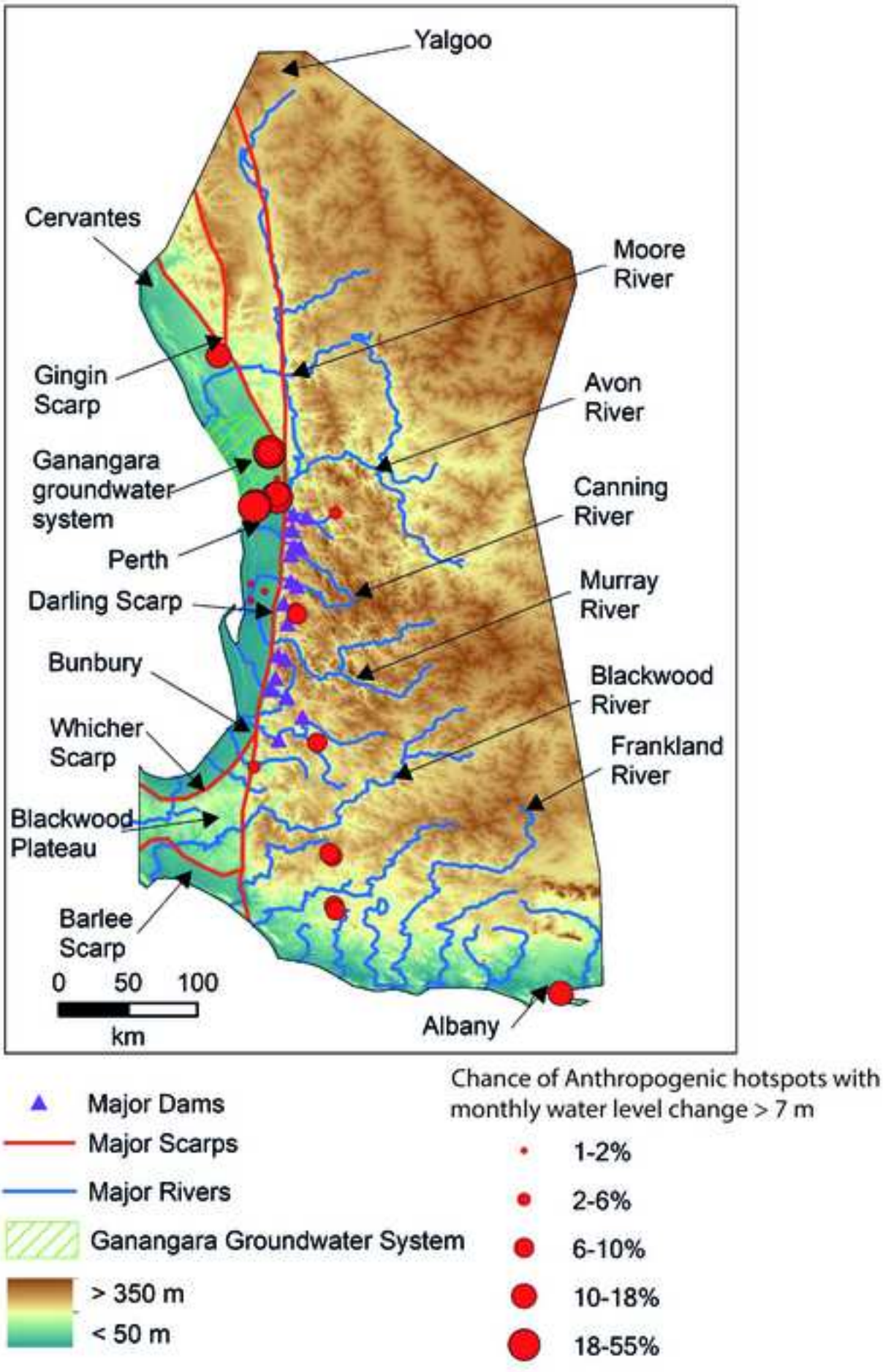

Figure 8

Click here to download high resolution image

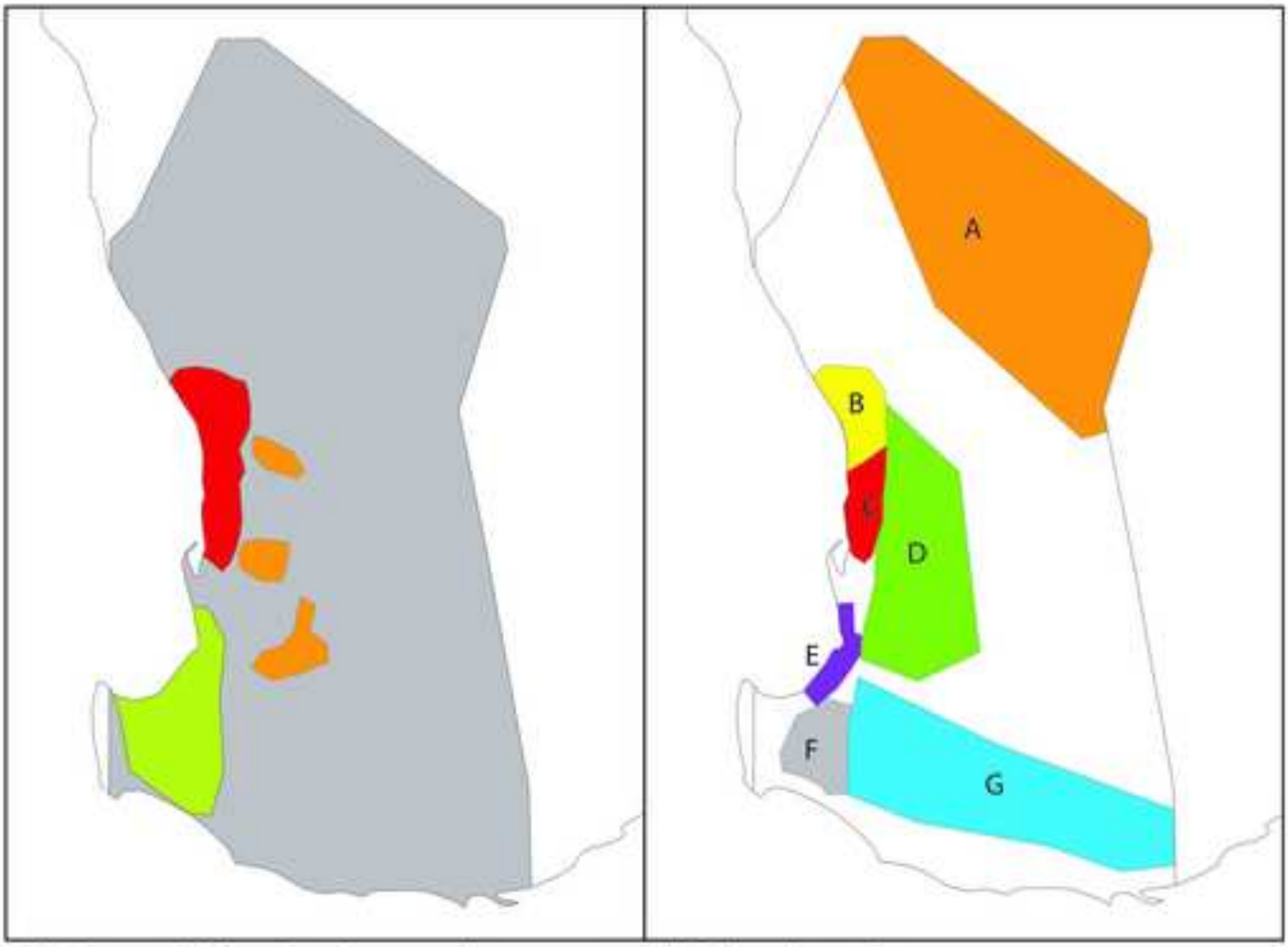

(a) Data spatial density and temporal coverage

(b) Sub study regions

- High density, long period of coverage
- High density, short period of coverage
- low density, long period of coverage
- low density, short period of coverage large uncertainty of interpolation

- North mountainous region
- North Perth
- South Perth
- Central mountainous region
- Bunbury
- Blackwood Plateau
- South mountainous region

Figure 9

Click here to download high resolution image